Variations in benthic foraminiferal assemblages in the Tagus mud belt during the last 5700 years: Implications for Tagus River discharge

Dessandier Pierre-Antoine[a,$], Bonnin Jérôme[a], Malaizé Bruno[a], Lambert Clément[b], Tjallingii Rik[c,#], Warden Lisa[c], Sinninghe Damsté Jaap S[c,d], Kim Jung-Hyun[c,§].

[a]*UMR-EPOC 5805 CNRS, Université de Bordeaux, Allée Geoffroy St. Hilaire, 33615 Pessac, France*

[b]*Lemar UMR 6539, Université de Bretagne Occidentale, IUEM Technopôle Brest-Iroise, rue Dumont d'Urville - 29280 Plouzané, France*

[c]*NIOZ Royal Netherlands Institute for Sea Research, Department of Marine Microbiology and Biogeochemistry, and Utrecht University, NL-1790 AB Den Burg, The Netherlands*

[d]*Utrecht University, Department of Geosciences, Faculty of Earth Sciences, PO Box 80.021, Utrecht, The Netherlands*

[$]*Current address: CAGE—Center of Arctic Gas Hydrate, Environment and Climate, Department of Geology, UiT University of Norway, Tromsø, Norway*

[#]*Current address: Climate Dynamics and Landscape Evolution, GFZ German Research Centre for Geosciences, Potsdam, Germany*

[§]*Current address: Korea Polar Research Institute, 26 Songdomirae-ro, Yeonsu-gu, Incheon 21990, South Korea*

*Corresponding author:

Email: pierre-antoine.dessandier@uit.no

Abstract

We analyzed a 10-m sediment core retrieved at 82 m water depth off the coast of the Tagus River (Western Iberian Margin, Portugal) to investigate a linkage between variations in benthic foraminiferal assemblages and Tagus River discharge over the last 5700 years. Benthic foraminiferal assemblages were studied at high resolution in combination with the stable carbon and oxygen isotopic composition of fossil shells of *Nonion scaphum*, bulk and molecular organic matter properties (TOC, TN, C/N ratio, $\delta^{13}C_{TOC}$, $\delta^{15}N_{bulk}$, and BIT index), magnetic susceptibility, and XRF analyses. Three periods of environmental changes were identified: 1) high Tagus River discharge in 5750-2200 calendar year before present (cal yr BP), 2) lower discharge characterized by intense upwelling conditions (2250-1250 cal yr BP), and 3) both intense upwelling and Tagus River discharge (1250 cal yr BP-present). The data reveal alternating intense upwelling periods, as shown by the dominance of *Cassidulina carinata*, *Valvulineria bradyana*, or *Bulimina marginata*, whereas periods of increased river discharge are indicated by increase of *N. scaphum*, *Ammonia beccarii*, and *Planorbulina mediterranensis*. The Tagus River discharge was the strongest during the first period, transporting riverine material further offshore and preventing the establishment of a mud belt on the mid-shelf (around 100 m depth). During the second period, a decrease in Tagus River discharge favored the formation of the Tagus mud belt and strongly influenced the benthic environment by creating an organic matter stock. During the third period, intense upwelling and increased Tagus River discharge were recorded by benthic foraminiferal distribution, with an increase of terrestrial elements present in the mud belt. Furthermore, our results showed that variations in benthic foraminiferal assemblages corresponded to the well-known climatic periods in the study area, such as the Roman Period, the Dark Ages, the Medieval Warm Period, and the Little Ice Age. Our study strongly suggests that benthic foraminiferal assemblages can be used as a bio-indicator to trace the influence of past river discharge.

27

1. Introduction

29   In the last decades, benthic foraminiferal assemblages have often been used in

30   paleoceanography to investigate biostratigraphy, paleobathymetry, and abiotic conditions, such

31   as temperature, salinity, and pH (Jorissen et al., 2007 and references therein). The TROX model

32   (Jorissen et al., 1995) established that oxygen concentration and organic matter content in the

33   sediment are the major environmental controls on the distribution of benthic foraminifera in

34   marine sediments. Subsequent studies emphasized the importance of the quality of the organic

35   matter for the composition of living benthic foraminifera faunas in various marine environments

36   (e.g., Goldstein and Corliss, 1994; Suhr et al., 2003; Fontanier et al., 2005, Goineau et al., 2011,

37   Dessandier et al., 2015). Benthic foraminifera are known to bloom following high marine algal

38   production (e.g., Kitazato et al., 2000). After a phytoplankton bloom, benthic foraminifera

39   respond rapidly to the increased influx of fresh organic matter (Fontanier et al., 2003).

40   Terrestrial input may also impact the organic matter supply and its quality and thereby may

41   partly control the benthic foraminiferal distribution in continental shelf sediments. This is

42   particularly true for river-dominated shelves where living benthic foraminifera have been

43   identified to respond to river inputs (e.g., Mendes et al., 2004; Mojtahid et al., 2009; Goineau

44   et al., 2011).

45   Dessandier et al. (2016, 2018) have shown through studies on living and dead faunas

46   that some species could be used as bio-indicators of river discharge and upwelling intensity in

47   the Portuguese Margin. During the last millennia, these environmental conditions were

48   influenced by rapid climatic changes (Abrantes et al., 2005, Lebreiro et al., 2006). Within the

49   Quaternary, the Holocene is characterized by relatively stable climatic conditions with

50   millennial-scale variability (Bond et al., 1997). The solar variability superimposed on long-term

changes in insolation seems to be one of the most likely important forcing mechanisms for the rapid climate changes over the Holocene (Mayewski et al., 2004). The North Atlantic Oscillation (NAO) was also described as a major factor for the variability of climate in Europe (Wanner et al., 2001), which played an important role in the control of the upwelling intensity and humidity of the Iberian Peninsula (Abrantes et al., 2005; Lebreiro et al., 2006; Fig. 1). The NAO is an atmospheric process characterized by a seesaw between the Icelandic low and the Azores high pressures. The positive mode (NAO+) is characterized by well-developed Icelandic low and Azores high pressures, associated with stronger westerlies over the eastern North Atlantic and the European continent. The negative mode (NAO-) is characterized by a rather weak pressure seesaw and reduced westerlies (Wanner et al., 2001). The last millennia were marked by short-scale climatic changes, mainly controlled by solar activity and NAO-like processes. Several such periods of short-scale changes were identified, among them the Roman Period (RP; e.g., Lamb, 1985), the Dark Ages (DA; e.g., Keigwin and Pickart, 1999), the Medieval Warm Period (MWP), the Little Ice Age (LIA; deMenocal et al., 2000; Trouet et al., 2009), and a warming during the twentieth century determined by instrumental temperature measurements of the last two centuries. The major climatic changes, MWP and LIA, have been described as controlled by NAO+ and NAO-, respectively (Lebreiro et al., 2006; Trouet et al., 2009). The nature and chronology of these events are still debated (Desprat et al., 2003; Ortega et al., 2015; Swingedouw et al., 2015), but the influence of these abrupt changes on the rainfall and upwelling intensity has been observed in the Iberian Margin (Abrantes et al., 2005; Bartels-Jónsdóttir et al., 2006). During the NAO- mode, the Iberian Margin is marked by increased humidity, which is responsible for strengthened riverine discharge (Bernárdez et al., 2008). The NAO+ mode is characterized by an increase in Iberian coastal upwelling (Lebreiro et al., 2006). Another oscillation, called the Atlantic Multidecadal Oscilllation (Kerr, 2000), was also

75   described as a controlling factor of rainfall during the last century that had a greater influence

76   on the American continent, Sahel, and northern Europe (Knight al., 2006).

77   We tested the applicability of these benthic foraminifera as bio-indicators of past

78   upwelling intensity and changes in river discharge on a late Holocene sediment sequence from

79   the Tagus prodelta. We used a multiproxy approach based on organic parameters (total organic

80   carbon [TOC], total nitrogen [TN], C/N ratio, $\delta^{15}N_{bulk}$, and $\delta^{13}C_{TOC}$), XRF data, benthic

81   foraminiferal assemblages, and carbon and oxygen stable isotopes of benthic foraminifera to

82   compare climatic changes of the late Holocene with river regime change. The branched

83   isoprenoid tetraethers (BIT) index was measured in the core that was previously published in

84   Warden et al. (2016) and compared with our reconstruction. We applied our reconstruction on

85   a paleoclimatological record never studied at this water depth, under the influence of the Tagus

86   River, and provided a new dataset to improve understanding of the effect of NAO-like processes

87   during the Holocene.

88

89   **2. Study area**

90   Our study area was located at the mid-shelf off the Tagus River mouth, on the western

91   Iberian Margin (Fig. 1) which is a narrow (20–34 km) shelf (Dias et al., 2002) that extends from

92   37ºN to 42ºN latitude. The shelf break is located at 140 m depth, on the outer continental shelf

93   and slope, and three main submarine troughs (the Cascais Canyon, Lisbon Canyon, and Setùbal

94   Canyon) are related to geological features (Jouanneau et al., 1998). The regional hydrodynamic

95   regime is driven by the influence of wave action, tidal and rip currents, and storm surges, which

96   plays a role in determining the particle size distribution on shelf sediments (Oliveira et al.,

97   2007). However, the Tagus area is protected against swell from the northwest (Jouanneau et al.,

98   1998). Sandy deposits occur on the inner shelf, where there are high-energy littoral currents.

99   The dominant regional surface current (the Portugal Coastal Counter Current) flows southward

and transports material from the shelf to the deep ocean during winter storms (Vitorino et al., 2002b). The outer shelf is affected by internal waves, especially during periods when water masses are stratified, resulting in the deposition of large bodies of sandy and gravelly sands (Jouanneau et al., 1998). The export of terrestrial sediment and nutrients along the shelf is predominantly influenced by sediment supplied by three main rivers: the Douro, Tagus, and Sado (Jouanneau et al., 1998; Dias et al., 2002). At around 100 m water depth, the finest particles are deposited in accumulation areas, called the mud belt (or mud patch). The mud belt lies beyond the line where seasonal thermal stratification of surface waters occurs, especially off the mouths of the Douro and Tagus rivers (Jouanneau et al., 1998; Dias et al., 2002). These accumulation zones are composed of mixed sources of marine, estuarine, and terrestrial organic matter (Schmidt et al., 2010). Winter storms can remobilize the sediment and transport it northward by the action of bottom currents (Dias et al., 2002; Vitorino et al., 2002a), eventually depositing it on the mid-shelf mud belt between 50 and 130 m water depth (Vitorino et al., 2002b).

The Eastern North Atlantic Central Water (ENACW) is a slope current characterized by a decrease of salinity under the surface currents, with a minimum of 35.6 at 450–500 m water depth (Oliveira et al., 2007). The ENACW is upwelled during summer. Between May and September, the Azores high-pressure system is driven closer to the coast. Together with the associated northerly winds, this atmospheric system makes the colder, less salty, and nutrient-enriched subsurface water (60–120 m water depth) rise to the surface along the Iberian Margin (Fiúza, 1983). This upwelling leads to an increased productivity in the summer along a 50-km-wide zone. The main upwelling front is oriented along the bathymetry off the 100 m isobath in the northern part of the Iberian Peninsula; it then turns slightly offshore and southward (Peliz et al., 2002). Most of the primary producers, especially cyanobacteria and diatoms, that are dominant in the Iberian Margin increase during upwelling events (Tilstone et al., 2003). Active

upwelling periods have a large impact on marine trophic conditions in this area (Fiúza, 1983)

and are characterized by maximal organic carbon exports to the seafloor (Jouanneau et al.,

1998). Periods of strong Iberian river discharge that occur during phases when upwelling is

reduced are characterized by a substantially increased export of continental nutrients, which

triggers phytoplankton production (Prieto et al., 2009; Rodrigues et al., 2009). To a lesser

extent, phytoplanktonic blooms occur in November and between April and May (Ferreira and

Duarte, 1994). In winter, the Azores high-pressure system moves south, which results in

southerly winds and downwelling conditions that lead to the deposition of sediments on the

shelf (Frouin et al., 1990). Upwelling activity and fluvial discharge are consequently the two

major parameters controlling the marine biology on the Iberian Shelf (Lebreiro et al., 2006) due

to their impact on the deposition of organic matter, which is important for benthic organisms.

The Tagus is the longest (1,008 km) Iberian river in the central part of the Peninsula and

has a large mesotidal estuary with an area of 340 km^2 (Vale and Sundby, 1987). The Tagus

watershed is about 80,600 km^2 and has an annual mean water discharge of 360 m^3 s^{-1} (Jouanneau

et al.,1998), with strong seasonal changes in discharge from 1 to 2,200 m^3 s^{-1} (Atlas Nacional

de España), controlled by maximal rainfall in winter (Aguiar and Ferreira, 2005; Azevedo et

al., 2008). The Tagus River flows were largely modulated by the NAO during the last century

(Trigo et al., 2004) and the last millennia (e.g., Abrantes et al., 2005; Bartels-Jónsdóttir et al.,

2006; Lebreiro et al., 2006). The river discharge also controls the input of chlorophyll

associated with phytodetritic material in the marine environment and the water column

stratification (Relvas et al., 2007).

3. Material and methods

Core 64PE332-30-2 was obtained in March 2011 during the Pacemaker 64PE332 cruise

on board the R/V *Pelagia* (38°39'04''N, 9°28'13''W). This 978-cm Kullenberg piston core

150   was retrieved from the Tagus mud belt at 82 m water depth (Fig. 1). Sediment slices 1 or 2 cm

151   thick were sampled every 10 cm, dried, weighted, and washed through 63 and 150 µm sieves.

152   For this study, 101 samples of >150 µm benthic foraminifera were handpicked and placed in

153   Chapman cells before taxonomic identification under a stereomicroscope. After splitting using

154   an Otto microsplitter, a minimum of 250 specimens were counted. Diversity indices (Shannon

155   [S] and Evenness indices) were calculated using the PAleontological STatistics (PAST)

156   software (Version 2.14; Hammer et al., 2001). The benthic foraminiferal number (BFN), which

157   represents the number of individuals per analyzed dry sediment mass, was calculated for all

158   samples.

159   Isotopic analyses were performed on monospecific samples of the benthic foraminiferal

160   species *Nonion scaphum*, which is present all along the core and is typical of the Iberian mud

161   belt (Dessandier et al., 2015; 2016), at the EPOC laboratory, University of Bordeaux. This

162   species was observed alive below the oxygen penetration, between 1 and 2 cm depth in the mud

163   belt area (Dessandier et al., 2016), suggesting that it may reflect subsurface sediment pore water

164   rather than bottom water conditions. However, we compared only the data measured on the

165   same species in every sample, avoiding any bias from the early diagenesis effect for

166   environmental reconstruction. For each sample, three or four specimens were handpicked and

167   dissolved in acid via the Micromass Multiprep autosampler system. The resulting carbon

168   dioxide gas was analyzed against the international reference standard NBS 19 (δ^{13}C = + 1.96

169   ‰ / PDB and δ^{18}O = − 2.20 ‰ / PDB) using an Optima Micromass mass spectrometer.

170   Measurements were taken for each depth horizon (1 cm) in triplicate to reduce uncertainties.

171   The analytical precision was better than 0.05 ‰ for δ^{18}O and 0.03 ‰ for δ^{13}C.

172   The age model for the sediment core, modified according to Warden et al. (2016), was

173   based on the magnetic susceptibility (MS) and seven accelerated mass spectrometry (AMS) ^{14}C

174   radiocarbon dates (Table 1). The MS record of Core 64PE332-30-2 was compared with that of

175   Core GeoB 8903 (Abrantes et al., 2008), which was also retrieved in the Tagus prodelta at ~100

176   m water depth (Fig. 1). Table 1 summarizes the ^{14}C AMS dating points of the two cores

177   considered in this study. Because of the low number of dating points in the upper part of Core

178   64PE332-30-2, we compared our record of MS and age model with Core GeoB 8903, which

179   had a substantial number of ^{14}C AMS dating points in the upper section (Figs. 2 and 3). The

180   MS was measured on board at 5-cm intervals using a Bartington MS meter with a 12-cm

181   diameter loop. The final age model was achieved by a linear interpolation between each AMS

182   ^{14}C age. The ^{14}C data calibration was made via the program CALIB V0.6 with the Marine13

183   calibration curve (Stuiver and Reimer, 1993), using the common reservoir age of 400 years

184   because no regional effect on reservoir age is known in our sampling area (Abrantes et al.,

185   2005). AMS ^{14}C ages and the dating points of GeoB8903 were converted to cal yr BP.

186   Core 64PE332-30-2 was scanned with an Avaatech XRF core scanner at NIOZ at 1-cm

187   resolution. Detailed bulk-chemical composition records acquired by XRF core scanning allow

188   accurate determination of stratigraphical changes and assessment of the contribution of the

189   various components in lithogenic and marine sediments (Stuut et al., 2014). The XRF core

190   scanner uses energy dispersive fluorescence radiation to measure the chemical composition of

191   the sediment as element intensities in total counts or counts per second (Tjallingii et al., 2007).

192   After cleaning and preparation of the archive-halve core surface and covering with SPEX Certi

193   Ultralene$^{®}$ foil, the core was measured at both 10 kV and 30 kV. Element intensities are

194   presented as log ratios that are normally distributed and linearly related to log ratios of element

195   concentration (Weltje and Tjallingii, 2008). Terrestrial exports, such as metals or contaminants,

196   are indicated mainly by Fe/Ti and Pb/Ti ratios. The Zr/Rb ratio serves as a grain size indicator

197   (Taylor, 1965), and the Br/Cl ratio indicates organic sediment (Ziegler et al., 2008).

198   Sediments were freeze-dried and ground before the geochemical analyses. TN and δ^{15}N

199   were measured with a Thermo-Scientific Flash 2000 Elemental Analyzer interfaced at NIOZ.

200 The analyses were determined at least in duplicate and the analytical error was, on average,

201 smaller than 0.1 wt. % for the TN content. The TOC content, the stable carbon isotopic

202 composition of TOC ($\delta^{13}C_{TOC}$), and BIT data were previously published by Warden et al.

203 (2016). The C/N ratio was calculated as the division of TOC/TN.

204   A principal component analysis (PCA) was performed on 22 samples of normalized

205 environmental and faunal data, using PRIMER version 6.0 software (Clarke and Warwick,

206 1994) to compare the response of the faunal and environmental parameters. The two major PCA

207 scores were plotted to define the different phases of the reconstruction.

208

209 **4. Results**

210 <u>4.1. Sedimentological features and age model</u>

211   The final age model of Core 64PE332-30-2 (Fig. 3) revealed that the sedimentation rates

212 were increasing over time, with a first phase of ~0.06 cm/yr^{-1} from 5750 to 2200 cal yr BP. In

213 a second phase, 2200-present, the sedimentation rate was ~ 0.52 cm yr^{1}. The MS record and

214 grain size distribution of the Core GeoB 8903 were plotted as a function of age, and the MS

215 and Ca/Ti record of Core 64PE332-30-2 were plotted as a function of core depth (Fig. 2).

216 Similar trend signals in the MS records were identified in the two cores, and the Ca/Ti record

217 measured by XRF showed a similar trend to the grain size record of core GeoB 8903. The MS

218 record showed three phases, with the first characterized by an increase of MS at 770 cm

219 sediment core depth, the second a larger increase at around 400 cm, and the third a more stable

220 trend until the end. This trend was opposite that of the Ca/Ti content, which revealed two

221 successive decreases of values at the same depths.

222

223 <u>4.2. Environmental change phases</u>

XRF, organic matter, and benthic foraminiferal isotopes data are plotted in Fig. 4. Three phases appeared following the environmental changes, mainly determined by the XRF ratios. Phase I (575-2250 cal yr BP) was characterized by high Zr/Rb and Ca/Ti counts, while the Br/Cl and Fe/Ti counts were low. The BIT index was low and stable (below ~ 0.04), the TOC content was also stable at around 0.9 wt. %, $\delta^{13}C_{TOC}$ was about − 24.3 ‰, and $\delta^{15}N_{bulk}$ was about + 3.9 ‰ (Warden et al., 2016). The TN was the only organic parameter that slightly increased during this phase, from 0.04 to 0.08 wt. % (Warden et al., 2016). The C/N ratio showed an opposite trend, with a clear decrease from 18 to 11. Both the carbon and oxygen stable isotope composition of *N. scaphum* slightly decreased during this interval, $\delta^{18}O_{bf}$ from + 1.7 to + 1.4 ‰ and $\delta^{13}C_{bf}$ from − 1.1 to − 1.2 ‰.

Phase II (2250-1250 cal yr BP) was characterized by a rapid decrease in Ca/Ti and Zr/Rb counts, a strong increase in Br/Cl counts, and a slight increase in Fe/Ti. The BIT index increased slightly, to 0.06. The TOC, $\delta^{13}C_{TOC}$, and C/N ratio reached high values at the end of the period (around 1.5 wt. %, − 23.0 ‰, and 16, respectively) after a large increase. TN and $\delta^{15}N_{bulk}$ showed a smaller increase; TN moved from 0.9 to 0.13 wt. % and $\delta^{15}N_{bulk}$ from + 3.6 to + 3.9 ‰. Isotopes measured on benthic foraminifera became more variable at the beginning of the period, and this trend continued until the end of the record. The decrease in δ^{13}_{bf} observed in phase I was stronger, and $\delta^{18}O_{bf}$ remained fairly constant.

Phase III (1250 cal yr BP-present) was characterized by a continued decrease of Ca/Ti counts and a large decrease of Zr/Rb counts. Br/Cl counts were also unstable and lacking any clear trend. The Fe/Ti and Pb/Ti counts from Phase III showed an increase until the end of the record, especially during the last 500 years for Pb/Ti, after a stable trend during the two previous phases. They both peaked at 250 cal yr BP, when Br/Cl decreased. The TOC content, $\delta^{13}C_{TOC}$, and C/N ratio decreased, to 1.2 wt. %, − 24 ‰, and 8, respectively. The $\delta^{13}C_{TOC}$ and TOC increased during the last 200 years, reaching − 28.8 ‰ and 1.2 wt. %, respectively. TN and

249    $\delta^{15}N_{bulk}$ were roughly constant before a large increase at the end of the period, reaching 0.17 %

250   and + 4.7 ‰, respectively. The $\delta^{18}O_{bf}$ increased at the beginning from + 1.3 to + 1.8 ‰ and

251   decreased until + 1.5 ‰ at the end; $\delta^{13}C_{bf}$ showed the opposite trend, with a large decrease from

252   − 1.5 to − 3.5 ‰. The C/N ratio was slightly decreasing from the start of this period until the

253   present. Conversely, the BIT index was progressively increasing, reaching 0.12, but dropped in

254   the most recent sediment horizon analyzed.

255

256   4.3. Benthic foraminiferal distribution over the last 5750 years

257   Fig. 5 shows percentages of the major species (> 5 %). Based on the distribution of these

258   dominant taxa, three different phases could be identified. The first phase does not map to the

259   environmental phases and ends at 2500 cal yr BP. During this phase (5750-2500 cal yr BP), *N.*

260   *scaphum* and *Ammonia beccarii* dominated, making up 30 and 18 % of the total species,

261   respectively. *Planorbulina mediterranensis* and *Bolivina spathulata* were relatively abundant

262   as well, with each ~10 % of the population. *A. beccarii* was particularly dominant (10-20 %)

263   between 5750 and 4750 cal yr BP and then quickly decreased to ~ 5 %. The epibenthic species

264   *Cibicides lobatulus* was only > 5 %, while *Hyalinea balthica* and *Uvigerina bifurcata* increased

265   until the end of the period. This first period was marked by a progressive increase of specific

266   richness; the S index increased from 28 to 36, and H' from 2.3 to 2.8. The foraminiferal density

267   (BFN) was relatively low during this period.

268   Between 2500 and 1250 cal yr BP, *Cassidulina carinata* increased sharply, while *N.*

269   *scaphum* clearly decreased in relative abundance. *Valvulineria bradyana* was nearly absent

270   during the first phase but became abundant from 2250 cal yr BP and reached 10 % of the fossil

271   assemblage during the latter period of this second phase. Smaller variation in the relative

272   abundances of the other dominant species, such as *P. mediterranea*, *A. beccarii*, *H. balthica*,

273   and *U. bifurcata*, was observed without a clear trend. *V. bradyana* and *Bulimina marginata*

274 increased, and *C. lobatulus* and *B. spathulata* diminished. The highest percentages of *C.*

275 *carinata* (40 %) were observed between 1750 and 1500 BP, whereas *Bulimina marginata*, *P.*

276 *mediterranensis*, and *B. spathulata* decreased. The BFN increased as both specific richness and

277 the S index began an initial decline; specific richness was decreasing until 30 taxa, and H' until

278 2.5.

279   The last phase (1250 cal yr BP-present, Phase III) was characterized by higher relative

280 abundance of *V. bradyana*, dominance of *C. carinata*, and a progressive decrease of *P.*

281 *mediterranensis*, *A. beccarii*, and *B. spathulata.* The relative abundance of *N. scaphum* slightly

282 increased from 1250 cal yr BP, compared to 2600-1250 cal yr BP, but decreased again from

283 500 cal yr BP. After 1000 cal yr BP, a strong increase was recorded for *C. carinata*, to more

284 than 40 % at 500 cal yr BP and in the modern period. Deep infaunal species (i.e., *Chilostomella*

285 *oolina* and *Globobulimina affinis*), *B. marginata*, and *Eggerelloides scaber* also increased

286 during this phase. The last 200 years showed strong abundances of *C. carinata* (44 %) and a

287 large loss of both *V. bradyana* and *N. scaphum,* which decreased to ~ 10 %. *Bolivina spathulata*

288 and *H. balthica* totally disappeared, while *U. bifurcata*, *A. beccarii*, and *B. marginata* declined.

289 With *C. carinata*, only *B. aculeata* and *E. scaber* are increasing during this modern period. The

290 last 750 years showed a large decline of BFN, specific richness (~ 20), and S index (~ 2).

291

292 4.4. Multiproxy approach

293   A PCA was performed on the major environmental parameters (TOC, TN, $\delta^{13}C_{TOC}$,

294 $\delta^{15}N_{bulk}$, BIT index, Ca/Ti, Fe/Ti, Br/Cl, Zr/Rb, and benthic foraminiferal stable isotopes) and

295 on the relative abundances of the major benthic foraminiferal species (*C. carinata*, *N. scaphum*,

296 *V. bradyana*, *A. beccarii*, *P. mediterranensis*, *B. spathulata*, *E. scaber*, *H. balthica*, *U.*

297 *bifurcata*, *B. marginata*, and deep infaunas) (Fig. 6A). PC1 and PC2 explained 64 % (52 and

298 12 %, respectively) of the total variance observed in the dataset. The relative abundance of *N.*

299   *scaphum*, *A. beccarii*, and *P. mediterranensis* loaded positively on PC1 and negatively on PC2,

300   together with $\delta^{13}C_{bf}$, Ca/Ti, and Zr/Rb. Most organic compounds, such as TOC, TN, $\delta^{13}C_{TOC}$,

301   and $\delta^{15}N_{bulk}$, loaded negatively on PC1 and PC2 with *C. carinata*, Br/Cl, and Pb/Ti. The deep

302   infaunas and *B. marginata*, *V. bradyana*, and *E. scaber* loaded negatively on PC1 and positively

303   on PC2, together with Fe/Ti and the BIT index. *Uvigerina bifurcata*, *H. balthica*, and *B.*

304   *spatulata* loaded positively on PC1 and PC2 with $\delta^{18}O_{bf}$.

305   The scores of the different samples on PC1 and PC2 were plotted as a function of age

306   in Fig. 6B. The score of PC1 was stable during the first phase and then showed a slight increase

307   from 2500 to 2250 cal yr BP. At the start of Phase II (2250 cal yr BP), the score of PC1

308   decreased until 1500 cal yr BP, then increased again. At the start of Phase III (1250 cal yr BP),

309   a second progressive decrease started and characterized this phase until the present. The plot of

310   PC2 showed an increase toward positive loading until the end of phase I. The second phase

311   (2250-1250 cal yr BP) was characterized by a sharp decrease, before an increase at the

312   beginning of Phase III that continued until 750 cal yr BP. PC2 decreased, reaching 0 at 500 cal

313   yr BP, showed a slight increase between 500 and 250 cal yr BP, and decreased again during the

314   last period of Phase III.

315

316   **5. Discussion**

317   5.1. Benthic foraminiferal response to environmental and climatic changes

318   Climatic changes during the late Holocene have been well studied in the Portuguese

319   Margin, especially for the last 3000 years (e.g., Desprat et al., 2003; Abrantes et al., 2005;

320   Bartels-Jónsdóttir et al., 2006; Alt-Epping et al., 2009). This rendered the Holocene a suitable

321   period to test benthic foraminifera as bio-indicators for past Tagus River discharge and

322   environmental changes based on the living foraminiferal calibration developed by Dessandier

323   et al. (2016, 2018) in the same location. Previous sediment cores in the area extended back to

324   2000 (Abrantes et al., 2005; Bartels-Jónsdóttir et al., 2006) or 3000 cal yr BP (Alt-Epping et

325   al., 2009). The 10-m core retrieved in our study provided a record that dated to 5750 cal yr BP.

326   Next, we present the three phases defined by environmental changes related to sediment

327   supplies, as shown by the XRF ratios and visible in the scores of the PCA (Fig. 6B).

328   The first phase was characterized by positive values of PC1 and a continuous increase

329   in PC2, starting from negative values. The Zr/Rb ratio indicates a bigger grain size, which had

330   a strong positive loading on PC1 together with Ca/Ti. Ca was previously linked to grain size in

331   the Portuguese Margin and thought to be associated with coarse reworked shells of

332   macrobenthic organisms (Martins et al., 2007; Abrantes et al., 2008; Alt-Epping et al., 2009).

333   The two different increases of Zr/Rb and Ca/Ti were two successive phases in grain size

334   decrease from Phase I to Phase III (Fig. 4). During Phase I, the TOC content of the sediment

335   and the Br/Cl were very low; both indicated low amounts of organic compounds, likely because

336   of this coarse grain size. This phase was characterized by river-influenced species, such as *N.*

337   *scaphum*, *A. beccarii*, and *P. mediterranensis*. This first group of species consequently

338   represents the river discharge bio-indicator in this study. Among them, *N. scaphum* was

339   interpreted as an indicator of active upwelling conditions in previous studies of the Portuguese

340   Margin (Bartels-Jónsdóttir et al., 2006). However, the results from late winter showed that this

341   species was clearly dominant in the living community of the Portuguese inner shelf during

342   winter. By contrast, during active upwelling context, it was present only in the dead community,

343   reflecting lower relative abundances (Dessandier et al., 2016; 2018). The large occurrences of

344   *A. beccarii* and *P. mediterranensis* during this first phase indicated strong bottom currents and

345   coarse sediments (e.g., Murray, 2006; Schönfeld, 2002), whereas *C. lobatulus* was previously

346   believed not to be endemic to this study area (Dessandier et al., 2018). The presence of the latter

347   was probably an indicator of transport from the estuary to the shelf, as this species is typically

348   found in Portuguese estuaries (Martins et al., 2015). The dominance of *N. scaphum* and *A.*

beccarii further suggested inputs from the estuary of phytoplankton or nutrients that may boost local marine productivity, such as coccolithophores, as has been previously observed where the Douro River flows into the ocean, where these species dominated the living fauna in late winter (Dessandier et al., 2015). This may indicate an influx of relatively labile organic matter, consistent with the progressive increase of faunal diversity during this period.

The second phase began with the Tagus mud belt establishment at around 2250 cal yr BP, which was represented by the plot of PC1, when the Ca/Ti and Zr/Rb counts clearly decreased and terrestrial elements (Fe/Ti, Pb/Ti, and BIT index, Fig. 4) increased. This suggests a deposition of finer sediments of terrestrial origin in the Tagus prodelta during this period. This important change in sedimentary conditions toward muddier and organic-rich sediment (Martins et al., 2006) was observed in the Portuguese Margin earlier, at around 2000 cal yr BP (Alt-Epping et al., 2009; Martins et al., 2007), and indicated the onset of the Tagus mud belt, which was mainly composed of sediment exported from the Tagus estuary (Jouanneau et al., 1998). This increase of organic compounds was also highlighted by the large increase in the Br/Cl ratio during this phase. The reduction of bottom water currents driven by decreasing wind and more humid conditions have been postulated as the physical processes that triggered a strong Tagus River export of sediment and led to the formation of the mud belt around this time (Alt-Epping et al., 2009). The mud belt formation was responsible for the increased accumulation of organic matter, especially during Phase II, corresponding to the increased levels of Br/Cl, TOC, and TN content (Fig. 4). The strong negative loading of both $\delta^{13}C_{TOC}$ and TOC on PC2 might suggest that the major supply of organic matter was driven by marine production, particularly during the strong upwelling conditions that characterized Phase II. The $\delta^{18}O_{bf}$ in this area was primarily controlled by salinity, with a reduced temperature effect, showing an increase in salinity during upwelling events (Lebreiro et al., 2006). This phase was characterized by a large increase of *C. carinata*, *V. bradyana*, and *B. marginata* abundances,

374   indicating that higher trophic levels occurred in the sediments, caused by high organic matter

375   content in the mud belt. In this area, the active upwelling period corresponds to the most

376   eutrophic conditions, mainly highlighted by the abundance of *C. carinata,* associated with

377   marine organic matter (Br/Cl and $\delta^{13}C_{TOC}$; Fig. 6). *Cassidulina carinata* was already interpreted

378   as highly dominant in an active upwelling context and adapted to cold, nutrient-rich waters

379   (Bartels-Jónsdóttir et al., 2006; Martins et al., 2006). Together with this species, *V. bradyana,*

380   *B. marginata, H. balthica*, and *U. bifurcate* have essentially been found only in the dead

381   community and with almost no occurrence in the late winter (Dessandier et al., 2016). The

382   increase in *V. bradyana* abundance correlated with the onset of Phase II and the mud belt. This

383   result corroborated this species' need for rich trophic conditions and suggested that the second

384   phase stabilized with the onset of strong upwelling conditions. *Nonion scaphum* and *V.*

385   *bradyana* were highly dominant during this interval, although *N. scaphum* was less abundant

386   than in Phase I. These two species live under organic-rich conditions and can tolerate anoxic

387   sediments (Fontanier et al., 2002; Barras et al., 2014), which may suggest that large terrestrial

388   inputs in this area led to periodic anoxia. The upwelling events create ideal environmental

389   conditions for diatom blooms that resulted in the presence of other species during summer

390   periods (Dessandier et al., 2016). This seasonal production indicated a preference of these

391   opportunistic species for summer periods, when the influence of upwelling is at its maximum.

392   During upwelling periods, diatoms are the major phytoplankton group responding to cold and

393   nutrient-rich ENACW. However, the preservation of this group as fossils is dependent on high

394   fluxes of individuals to the seabed (Abrantes et al., 1988), which constrains the use of this proxy

395   for environmental changes. Conversely, winter periods characterized by maximum continental

396   runoff had evidence of coccolithophore blooms, which responded to stratified waters (Abrantes

397   and Moita, 1999). Since phytoplanktonic groups favor certain environmental conditions, these

398   phytodetrital sources for benthic foraminifera may partially explain the seasonal variation in

species composition. This result may be the consequence of preferences for the specific component of seasonally deposited phytodetritus, as has been observed in the Antarctic (Suhr et al., 2003).

During Phases II and III, $\delta^{13}C_{bf}$, representing the exported phytodetritus to the seafloor (Curry et al., 1988), indicated higher primary production, whereas the increase of $\delta^{15}N_{bulk}$ may illustrate nutrient degradation or a stronger influence of estuarine sources of organic matter (Owens, 1985). Phase III was characterized by a change in organic matter sources from predominantly marine origin (negative loads on PC2) to predominantly terrestrial origin (positive loads on PC2). This period showed a drop in foraminiferal diversity corresponding to the dominance of *C. carinata* (up to 43 %). The increase in abundance of the deep infaunal species at around 1000 cal yr BP suggested this is when the enrichment in organic matter of the prodelta occurred and might indicate episodic periods of dysoxia or even anoxia related to potential eutrophication, such as the occurrence of *G. affinis* and *C. oolina*, well known to live in highly eutrophic conditions, often below the oxic sediments (Jorissen et al., 1998; Mojtahid et al., 2010a). The faunal evolution, in terms of assemblages and diversity within Phases II and III, revealed other controlling factors independent of the presence of the Tagus mud belt, represented by the PC2 (Fig. 6B). An increase in pollutants during this period was thought to occur concomitantly with the disappearance of *H. balthica* and appearance of *E. scaber*, as has been observed off Iberian rivers (Diz et al., 2002; Bartels-Jónsdóttir et al., 2006). The increase of pollutants indicated by the appearance of *E. scaber* also fits the results of Alve (1995), who described *E. scaber* as a pollution-tolerant species under aquaculture influence.

5.2. Reconstruction of environmental evolution in the Tagus prodelta during the last 5750 years

5.2.1. First phase (5750-2250 cal yr BP): High Tagus River discharge

423   The modern sediment cover in the Tagus prodelta is mainly supplied by terrestrial silts

424 and clays exported by Tagus River discharge (Jouanneau et al., 1998). The influence of sea

425 level changes on the Iberian Margin is no longer significant on the sedimentation after ~ 7000

426 yr BP (Vis et al., 2008). The sedimentary evolution of the Tagus prodelta was mainly controlled

427 by Tagus River discharge and impacted by climatic changes after this period. This area was

428 particularly characterized by very humid conditions between 6500 and 5500 yr BP,

429 corresponding to the African Humid Period (deMenocal et al., 2000; Renssen et al., 2006; Vis

430 et al., 2010). The coarse sediments observed during Phase I, highlighted by both environmental

431 and faunal evidence, are in good agreement with conditions described by Rodrigues et al.

432 (2009), who interpreted intense deforestation and soil destabilization as factors responsible for

433 the increased current velocity of the Tagus River. These coarse sediments with low organic

434 content and of marine origin were similar to sediments of modern inner shelf conditions

435 observed down to 50 m water depth in the Portuguese Margin (Schmidt et al., 2010). These

436 conditions are synthesized in Fig. 7A and demonstrate that when the Tagus River discharge was

437 large, it prevented any deposition of fine material on the mud belt, resulting in low

438 sedimentation rates. The fine sediment deposits of terrestrial origin were probably transported

439 further offshore during this phase. The position of Core 64PE332-30-2 might have been a zone

440 of fine sediment bypass similar to what is currently observed on the inner shelf. This explains

441 the low organic content, the low BIT index, and the $\delta^{13}C_{TOC}$ that signaled the marine origin of

442 the sediments. Similar conditions were observed for this period in the Galicia mud deposit

443 (Martins et al., 2007; Bernárdez et al., 2008) and off the Guadiana River (Mendes et al., 2010)

444 and were believed to indicate a strong hydrodynamic regime. Tagus River floods have been

445 reconstructed in the lower Tagus River valley between 4900 and 3500 yr BP and were

446 associated with strong deforestation during this period (Vis et al., 2010).

447   The transition between Phases I and II was marked by a shift between the faunal and

448   environmental signals, between 2600 and 2250 cal yr BP (Fig. 5). The species that first reacted

449   to this, *C. carinata*, started to increase in abundance, resulting in a decrease in the relative

450   abundances of the other species, including the taxa indicators of river discharge. This reflected

451   the very opportunistic nature of *C. carinata* and provided a more accurate signal of the

452   environmental change than the geochemical parameters, which merely recorded the mud belt

453   conditions. A progressive decrease of fluvial influence was visible following the strong decline

454   of *A. beccarii* and *N. scaphum,* which has also been observed during the last 3000 years within

455   the Ría de Vigo (Diz et al., 2002). This may be the transition between colder and wetter

456   Subboreal conditions and warmer, dryer Sub-Atlantic conditions at 3000 yr BP (Alt-Epping et

457   al., 2009; Bernárdez et al., 2008). The Sub-Atlantic period was associated with the reduced

458   influence of winds on the Iberian Margin (Martins et al., 2007), a reduction in hydrodynamic

459   marine currents, and the collection of fine sediments in the Galicia mud deposit. These

460   conditions were responsible for the lateral movement of the mud deposit on the shelf, with the

461   construction of the mud belt at the beginning of Phase II (2250 cal yr BP). The accumulation

462   of muddy sediments on the shelf off the Tagus River at ~ 2000 years BP was synchronous with

463   the establishment of the mud belt off the Douro River (Drago et al., 1998). This coordination

464   suggests a response to regional rather than local change in the climate, responsible for a dryer

465   period and an increase of clay accumulation closer to the Tagus River mouth, due to the

466   decrease in Tagus discharge.

467

468   5.2.2. Second phase (2250-1250 cal yr BP): High upwelling intensity

469   After the onset of the Tagus mud belt at ~ 2250 cal yr BP, two alternative regimes

470   prevailed, one characterized by intense upwelling and the other by strong river discharge, as

471   summarized in Fig. 7B. During this phase, TN, $\delta^{13}C_{bf}$, and $\delta^{15}N_{bulk}$ showed an increase in

472 productivity, probably due to a change in Tagus River flux conditions. However, this was not

473 recorded by all environmental parameters. The faunal results could indicate that the organic

474 matter supply during Phase II was related to upwelling events more than Tagus River inputs.

475 The decrease in the C/N ratio was not in agreement with $\delta^{13}C_{TOC}$ data, making it difficult to

476 evaluate the organic matter source. The $\delta^{13}C_{TOC}$ and the C/N ratio are often used to determine

477 the sources of organic matter (e.g., Hedges and Parker, 1976; Peters et al., 1978; Alt-Epping et

478 al., 2007). However, the C/N ratio is affected by the preferential remineralization of nitrogen in

479 marine sediments or nitrogen sorption onto clay minerals (Schubert and Calvert, 2001), and the

480 $\delta^{13}C_{TOC}$ signal could be from a mixture of C3 and C4 plants, mimicking the isotopic signal of

481 marine algae (e.g., Goñi et al., 1998). Both of these indicators in the paleorecords might be

482 affected by organic matter degradation. Additionally, $\delta15N_{bulk}$ could be affected in the study

483 area by a higher influence of agriculture and pollution (Alt-Epping et al., 2009). Nevertheless,

484 $\delta^{13}C_{TOC}$ and the C/N ratio were useful to discriminate the marine and terrestrial sources of

485 organic matter in another study on the Portuguese Margin (Schmidt et al., 2010). In the present

486 study, only the C/N ratio seemed to be clearly affected by the early diagenesis. These organic

487 parameters were essential to compare the environmental signal with benthic foraminifera, and

488 their disagreement confirms the importance of using a multiproxy approach that included bio-

489 indicators that are less affected by organic matter degradation.

490   Phase II began at 2250 cal yr BP with a low amount of terrestrial input (indicated by the

491 negative loading of PC2; Fig. 6) and lasted until 1800 cal yr BP, which corresponded to the RP

492 (Lamb, 1985; Bernárdez et al., 2008). Despite the increase in eutrophy-tolerant species, the

493 faunal diversity and BFN were low at the beginning of the RP. The deposition of contaminants

494 and increased sediment accumulation rate may have limited faunal production during this

495 period. Lebreiro et al. (2006) also observed a large export of terrestrial particles into the Tagus

496 prodelta during the RP. This export was interpreted as a consequence of anthropogenic

activities, such as Roman gold mining, along the Tagus River. This export of terrestrial material may have been enhanced by the NAO- phase that occurred during that period and led to intensified rainfall in the Portuguese Margin (Abrantes et al., 2005). Periods of NAO- have strongly influenced Iberian river discharge, especially on the Tagus River (Trigo et al., 2004). The northern part of the Iberian Margin is marked by varying rainfall responses. This zone, which is very close to the limit of the NAO influence, is known to alternate between positive and negative correlation with the NAO and humid conditions (Alvarez and Gomez-Gesteira, 2006). Desprat et al. (2003) also identified warm and relatively humid conditions during the RP in the Ría de Vigo. A strong river regime such as this one was not observed off the Capbreton in the bay of Biscay (Mojtahid et al., 2009), suggesting an anti-correlation of the NAO phases between the two study areas.

The end of Phase II showed a decrease in the Tagus River influence that corresponded with an increase in positive loading of PC2, characterized by high marine organic matter content likely brought by active upwelling conditions. The increased abundance of *C. carinata* corroborated this context in the middle of Phase II, corresponding to a period of intense upwelling activity, which has also been described in the same area in a study using benthic foraminifera (Bartels-Jónsdóttir et al., 2006). The dominance of the opportunistic species *C. carinata* constrained faunal diversity, as observed in other studies (Fontanier et al., 2003; Dessandier et al., 2018). However, *C. carinata* did not increase until the end of Phase II, suggesting that the intensity of upwelling slowed down at the end of this phase. By contrast, the Tagus mud belt built up, allowing an increased deposition of marine organic matter until the end of Phase II. This difference could be the result of biased organic parameters (e.g., caused by early diagenesis). In addition, this study area was characterized by organic matter from different sources, which were recorded as a mixture of marine and terrestrial compounds by the organic parameters. What was revealed by the organic parameters as a record of upwelling

522 activity could instead result from high productivity throughout the entire year. Therefore,

523 benthic foraminiferal species recorded the organic matter sources more accurately.

524

525 5.2.3. Third phase (1250 cal yr BP-present): Alternating upwelling and Tagus discharge

526 influence

527   The beginning of Phase III (Fig. 7C), which corresponds to the DA, was followed by

528 the MWP, which occurred between 1100 and 600 yr BP, as reported in several studies

529 performed on the Portuguese Margin (e.g., Desprat et al., 2003; Rosa et al., 2007). The DA was

530 described as a period characterized by strong upwelling activity off the Douro River (Rosa et

531 al., 2007). The MWP is also well known in the Portuguese Margin as a period characterized by

532 active upwelling conditions triggered by NAO+ conditions (Abrantes et al., 2005; Bartels-

533 Jónsdóttir et al., 2006; Rosa et al., 2007; Rodrigues et al., 2009). The high primary productivity

534 was linked to upwelling events and created eutrophic conditions in sediments that allowed for

535 less competition among *B. spathulata*, *P. mediterranensis*, *Cribroelphidium gerthi*, and *H.*

536 *balthica*. This period, characterized by a warm and dry climate, was influenced by

537 anthropogenic activities and soil erosion (Rodrigues et al., 2009) that caused Fe and Pb to be

538 massively transported via Tagus River runoff to the prodelta. Dry soils restrained infiltration

539 and possibly triggered large flooding of the Tagus River (Benito et al., 2003). The increased

540 BIT index (Warden et al., 2016) and Fe/Ti and Pb/Ti ratios during the beginning of the MWP

541 suggested increased terrestrial input, corresponding with the increased loading of PC2 in the

542 first part of Phase III and the accumulation of finer sediments.

543   The LIA, between 600 and 100 yr BP, was characterized by the increase in terrestrial

544 material, as shown by the abrupt increase in the BIT index and Fe/Ti and Pb/Ti ratios at 250 cal

545 yr BP. This increase was also highlighted by the sharp decrease in PC2 (Fig. 6B), which could

546 be linked to the Lisbon earthquake in 1755 AD (200 cal yr BP; Abrantes et al., 2008) or to

massive exports of fine sediments from the Tagus River (low Zr/Rb). This period has been

described as characterized by abrupt cooling and wet conditions (Bradley, 2000). The LIA was

affected by high-frequency episodic Tagus River paleo-floods (Benito et al., 2003) and has been

associated with the transport of fine sediments from the continent via discharge from the Tagus

River under NAO- conditions (Abrantes et al., 2005; Bartels-Jónsdóttir et al., 2006). During the

LIA, an abrupt decrease in the abundance of *C. carinata* may indicate that a reduction in

upwelling conditions occurred. *V. bradyana*, *E. scaber*, *A. beccarii*, and deep infaunas

increased, possibly as a consequence of episodic anoxia and the presence of contaminants. The

presence of the deep infaunas that can tolerate refractory organic matter (Murray, 2006)

suggests a decrease in organic matter quality, as was also observed in the Galicia mud deposit

during this period (Martins et al., 2006). This decrease in quality may be the major cause of the

decreased infaunal diversity that occurred between 1000 cal yr BP and the present.

Nevertheless, the faunal results suggested that intense upwelling periods also occurred during

the LIA, as demonstrated by the increased abundance of *C. carinata*. This highlighted that this

period was unstable and characterized by several environmental changes. The results from this

study were in good agreement with previous studies in the same area for the last 2000 years

(Abrantes et al., 2005; Bartels-Jónsdóttir et al., 2006; Alt-Epping et al., 2009), except for small

time shifts in the upwelling versus Tagus River discharge periods corresponding to the

transition between Phases I and II. These time shifts could be the consequence of different age

models. Bartels-Jónsdóttir et al. (2006) demonstrated that an "intense upwelling period"

occurred, followed by a "very intense upwelling period" during the MWP, and finally a large

Tagus River discharge during the LIA, all determined through the analysis of benthic

foraminiferal distribution.

There were some differences during the MWP and the LIA between the reconstructions

from this study and the results from Bartels-Jónsdóttir et al. (2006). These variations could be

due to a different interpretation of certain species, specifically *N. scaphum,* which was determined to be controlled by upwelling in previous studies; by contrast, it was used as a river discharge proxy in this study, based on the ecological results from the study area (Dessandier et al., 2016). The use of environmental data combined with the composition of the major species in this study may allow a better interpretation of the mud belt onset than merely using benthic foraminiferal data. Our results were also in good agreement with the reconstruction of the Tagus River discharge and the upwelling strength reported in Abrantes et al. (2009).

Finally, during the last century, this area was contaminated by anthropogenic pollution, including numerous trace metals that were measured in excess in the Tagus estuary, such as AS, Pb, Zn, Cu, and Cd (Caçador et al., 1996; Jouanneau et al., 1998). The catchment area was also influenced by anthropogenic contaminants, such as domestic sewage and industrial wastes (e.g., petrochemistry, fertilizers, smelters; Carvalho, 1997). Our analyses were not performed to identify the sources of anthropogenic pollution; however, the XRF signal shows a clear increase of several contaminants (such as Pb) in the most recent interval. We do not have enough faunal resolution and environmental data to investigate the anthropogenic influence on benthic ecosystems, but we assume that the faunal assemblages respond to this anthropogenic activity, as shown in other environments (e.g., Alve, 1995). The faunal distribution shows increased abundances of deep infaunal species and of *E. scaber* but the disappearance of other species, such as *H. balthica*, as has already been observed as a consequence of anthropogenic pollution in the Tagus prodelta (Bartels-Jónsdóttir et al., 2006). The last century was also characterized by the construction of dams, which have likely influenced the sequestration of organic matter in the estuary and changed the influence of the Tagus River discharge on the shelf through increased input of finer material (Jouanneau et al., 1998) and increased correlation with NAO phases (Trigo et al., 2004), all of which could have significant environmental consequences that will be crucial to understand in the future.

6. Conclusions

The results of this study demonstrate the validity of using benthic foraminifera as bio-indicators of past river discharge and upwelling intensity in the Tagus prodelta during the last 5750 years. Major environmental changes, linked with late Holocene climatic variations, are summarized by key benthic foraminiferal taxa data in Fig. 8. This study showed an additional phase, between 5750 and 2250 cal yr BP, that has not yet been investigated in the Portuguese shelf. This phase was characterized by coarser sediment cover and dominated mostly by *N. scaphum* and *A. beccarii*, suggesting a very dynamic Tagus River system that facilitated the dispersion of coarse terrigenous particles onto the prodelta.

The progressive decrease of the Tagus River flow, resulting in the establishment of the modern Tagus mud belt, was the major process explaining the environmental changes that occurred before Phase II. The presence of a transition period (2500-2250 cal yr BP) at the end of Phase I was only supported by the composition of the benthic foraminifera; geochemical data did not reveal any environmental changes. This might be due to the extremely poor preservation of organic matter in coarse sediments (in which benthic foraminifera are fairly well preserved).

Phase II (2250-1250 cal yr BP) was characterized by fine continental deposits, responsible for a better food stock for benthic organisms throughout the record. This phase was marked by the increase of *C. carinata, V. bradyana*, and *B. marginata*, opportunistic species that mark the increase in upwelling intensity in this area, revealing the strongest upwelling activity during the DA and the MWP. The high organic matter stocks in the Tagus prodelta during this phase created more refractory organic matter, responsible for a faunal diversity decrease from 2250 cal yr BP to present.

Phase III (1250 cal yr BP-present) showed the disappearance of *B. spathulata*, *P. mediterranensis*, and *H. balthica* and the decrease of *A. beccarii* and *N. scaphum,* which may

622 be a consequence of a decrease in the organic matter quality and/or the occurrence of

623 anthropogenic pollution, as indicated by benthic foraminiferal assemblages and the XRF data.

624 Conversely, *E. scaber* increased, probably because of its pollution tolerance, and *C. carinata*

625 remained dominant, likely due to the strong upwelling conditions. Benthic foraminifera

626 responded accurately to record environmental and climate changes in the North Atlantic

627 continental shelf and therefore could be used as a bio-indicator of environmental changes, such

628 as changes in upwelling activity and river discharge, that were directly linked with the NAO.

629

641

642 **References**

643

644 Abrantes, F., 1988. Diatom assemblages as upwelling indicators in surface sediments off

645   Portugal. Mar. Geol. 85, 15–39.Abrantes, F., Moita, M.T., 1999. Water column and

646   recent sediment data on diatoms and coccolithophorids, off Portugal, confirm sediment

647   record of upwelling events. Oceanologica Acta 22, 67–84.

648 Abrantes, F., Lebreiro, S., Rodrigues, T., Gil, I., Bartels-Jónsdóttir, H., Oliveira, P., Kissel, C.,

649   Grimalt, J.O., 2005. Shallow-marine sediment cores record climate variability and

650   earthquake activity off Lisbon (Portugal) for the last 2000 years. Quaternary Science

651   Reviews 24, 2477–2494.

652 Abrantes, F., Alt-Epping, U., Lebreiro, S., Voelker, A., Schneider, R., 2008. Sedimentological

653   record of tsunamis on shallow-shelf areas: The case of the 1969 AD and 1755 AD

654   tsunamis on the Portuguese Shelf off Lisbon. Marine Geology 249, 283–293.

655 Aguiar, F.C., Ferreira, M.T., 2005. Human-disturbed landscapes: effects on composition and

656   integrity of riparian woody vegetation in the Tagus River basin, Portugal.

657   Environmental Conservation 32, 30–41.

658 Alt-Epping, U., Mil-Homens, M., Hebbeln, D., Abrantes, F., Schneider, R.R., 2007.

659   Provenance of organic matter and nutrient conditions on a river-and upwelling

660   influenced shelf: a case study from the Portuguese Margin. Marine Geology 243, 169–

661   179.

662 Alt-Epping, U., Stuut, J.-B.W., Hebbeln, D., Schneider, R., 2009. Variations in sediment

663   provenance during the past 3000 years off the Tagus River, Portugal. Marine Geology

664   261, 82–91.

665 Alvarez, I., Gomez-Gesteira, M., 2006. Influence of teleconnection patterns on precipitation

666   variability and on river flow regimes in the Miño River basin (NW Iberian Peninsula).

667   Clim Res 32, 63–73.

668 Alve, E., 1995. Benthic foraminiferal responses to estuarine pollution: a review. Journal of

669   Foraminiferal Research 25, 190–203.

670   Azevedo, I.C., Duarte, P.M., Bordalo, A.A., 2008. Understanding spatial and temporal

671   dynamics of key environmental characteristics in a mesotidal Atlantic estuary (Douro,

672   NW Portugal). Estuarine, Coastal and Shelf Science 76, 620–633.

673   Barras, C., Jorissen, F.J., Labrune, C., Andral, B., Boissery, P., 2014. Live benthic foraminiferal

674   faunas from the French Mediterranean Coast: towards a new biotic index of

675   environmental quality. Ecological Indicators 36, 719–743.

676   Bartels-Jónsdóttir, H.B., Knudsen, K.L., Abrantes, F., Lebreiro, S., Eiríksson, J., 2006. Climate

677   variability during the last 2000 years in the Tagus Prodelta, western Iberian Margin:

678   Benthic foraminifera and stable isotopes. Marine Micropaleontology 59, 83–103.

679   Benito, G., Sopeña, A., Sánchez-Moya, Y., Machado, M.J., Pérez-González, A., 2003.

680   Palaeoflood record of the Tagus River (central Spain) during the Late Pleistocene and

681   Holocene. Quaternary Science Reviews 22, 1737–1756.

682   Bernárdez, P., González-Álvarez, R., Francés, G., Prego, R., Bárcena, M.A., Romero, O.E.,

683   2008. Late Holocene history of the rainfall in the NW Iberian peninsula—Evidence

684   from a marine record. Journal of Marine Systems 72, 366–382.

685   Bond, G., Showers, W., Cheseby, M., Lotti, R., Almasi, P., Priore, P., Cullen, H., Hajdas, I.,

686   Bonani, G., 1997. A pervasive millennial-scale cycle in North Atlantic Holocene and

687   glacial climates. Science 278, 1257–1266.

688   Bradley, R.S., 2000. Enhanced: 1000 years of climate change. Science 288, 1353–1355.

689   Caçador, I., Vale, C., Catarino, F., 1996. Accumulation of Zn, Pb, Cu, Cr and Ni in sediments

690   between roots of the Tagus estuary salt marshes, Portugal. Estuarine, Coastal and Shelf

691   Science 42, 393–403.

692   Carvalho, F.P., 1997. Distribution, cycling and mean residence time of ^{226}Ra, ^{210}Pb and^{210}Po in

693   the Tagus estuary. Science of the total environment 196, 151–161.

694   Curry, W.B., Duplessy, J.-C., Labeyrie, L.D., Shackleton, N.J., 1988. Changes in the

695   distribution of $\delta13C$ of deep water $\Sigma CO2$ between the last glaciation and the Holocene.

696   Paleoceanography 3, 317–341.

697   Clarke, K. R., and R. M. Warwick (1994), Change in Marine Communities: An Approach to

698   Statistical Analysis and Interpretation, PRIMER-E Ltd.

699   Desprat, S., Sánchez Goñi, M.F., Loutre, M.-F., 2003. Revealing climatic variability of the last

700   three millennia in northwestern Iberia using pollen influx data. Earth and Planetary

701   Science Letters 213, 63–78.

702   Dessandier, P.-A., Bonnin, J., Kim, J.-H., Bichon, S., Grémare, A., Deflandre, B., de Stigter,

703   H., Malaizé, B., 2015. Lateral and vertical distributions of living benthic foraminifera

704   off the Douro River (western Iberian margin): Impact of the organic matter quality.

705   Marine Micropaleontology 120, 31–45.

706   Dessandier, P.-A., Bonnin, J., Kim, J.-H., Bichon, S., Deflandre, B., Grémare, A., Sinninghe

707   Damsté, J.S., 2016. Impact of organic matter source and quality on living benthic

708   foraminiferal distribution on a river-dominated continental margin: A study of the

709   Portuguese Margin. Journal of Geophysical Research: Biogeosciences 121, 1689–1714.

710   Dessandier, P.-A., Bonnin, J., Kim, J.-H., Racine, C., 2018. Comparison of living and dead

711   benthic foraminifera on the Portuguese Margin: understanding the taphonomical

712   processes. Marine micropaleontology 140, 1–16.

713   Dias, J.M.A., Jouanneau, J.M., Gonzalez, R., Araújo, M.F., Drago, T., Garcia, C., Oliveira, A.,

714   Rodrigues, A., Vitorino, J., Weber, O., 2002. Present day sedimentary processes on the

715   northern Iberian shelf. Progress in Oceanography 52, 249–259.

716   Diz, P., Francés, G., Pelejero, C., Grimalt, J.O., Vilas, F., 2002. The last 3000 years in the Ría

717   de Vigo (NW Iberian Margin): climatic and hydrographic signals. The Holocene 12,

718   459–468.

719   Drago, T., Oliveira, A., Magalhães, F., Cascalho, J., Jouanneau, J.-M., Vitorino, J., 1998. Some

720   evidences of northward fine sediment transport in the northern Portuguese continental

721   shelf. Oceanologica Acta 21, 223–231.

722   Ferreira, J.G., Duarte, P., 1994. Productivity of the Tagus estuary: an application of the EcoWin

723   ecological model. Gaia 8, 89–95.

724   Fiúza, A.F., 1983. Upwelling patterns off Portugal, in: Coastal Upwelling Its Sediment Record.

725   Springer, pp. 85–98.

726   Fontanier, C., Jorissen, F.J., Licari, L., Alexandre, A., Anschutz, P., Carbonel, P., 2002. Live

727   benthic foraminiferal faunas from the Bay of Biscay: faunal density, composition, and

728   microhabitats. Deep Sea Research Part I: Oceanographic Research Papers 49, 751–785.

729   Fontanier, C., Jorissen, F.J., Chaillou, G., David, C., Anschutz, P., Lafon, V., 2003. Seasonal

730   and interannual variability of benthic foraminiferal faunas at 550m depth in the Bay of

731   Biscay. Deep Sea Research Part I: Oceanographic Research Papers 50, 457–494.

732   Fontanier, C., Jorissen, F.J., Chaillou, G., Anschutz, P., Grémare, A., Griveaud, C., 2005. Live

733   foraminiferal faunas from a 2800m deep lower canyon station from the Bay of Biscay:

734   faunal response to focusing of refractory organic matter. Deep Sea Research Part I:

735   Oceanographic Research Papers 52, 1189–1227.

736   Frouin, R., Fiúza, A.F.G., Ambar, I., Boyd, T.J., 1990. Observations of a poleward surface

737   current off the coasts of Portugal and Spain during winter. Journal of Geophysical

738   Research 95, 679. doi:10.1029/JC095iC01p00679

739   Goineau, A., Fontanier, C., Jorissen, F.J., Lansard, B., Buscail, R., Mouret, A., Kerhervé, P.,

740   Zaragosi, S., Ernoult, E., Artéro, C., 2011. Live (stained) benthic foraminifera from the

741   Rhône prodelta (Gulf of Lion, NW Mediterranean): Environmental controls on a river-

742   dominated shelf. Journal of Sea Research 65, 58–75.

743   Goldstein, S.T., Corliss, B.H., 1994. Deposit feeding in selected deep-sea and shallow-water

744   benthic foraminifera. Deep Sea Research Part I: Oceanographic Research Papers 41,

745   229–241.

746   Goñi, M.A., Ruttenberg, K.C., Eglinton, T.I., 1998. A reassessment of the sources and

747   importance of land-derived organic matter in surface sediments from the Gulf of

748   Mexico. Geochimica et Cosmochimica Acta 62, 3055–3075.

749   Hammer, Ø., Harper, D.A.T., Ryan, P.D., 2001. Past: Paleontological Statistics Software

750   Package for education and data analysis. Paleontología Electrónica 4: 1-9. URL:<

751   http://palaeo-electronica. org/2001_1/past/issue1_01. html.

752   Hedges, J.I., Parker, P.L., 1976. Land-derived organic matter in surface sediments from the

753   Gulf of Mexico. Geochimica et Cosmochimica Acta 40, 1019–1029.

754   Jorissen, F.J., de Stigter, H.C., Widmark, J.G., 1995. A conceptual model explaining benthic

755   foraminiferal microhabitats. Marine Micropaleontology 26, 3–15.

756   Jorissen, F.J., Wittling, I., Peypouquet, J.P., Rabouille, C., Relexans, J.C., 1998. Live benthic

757   foraminiferal faunas off Cape Blanc, NW-Africa: community structure and

758   microhabitats. Deep-Sea Research Part I 45, 2157–2188.

759   Jorissen, F.J., Fontanier, C., Thomas, E., 2007. Paleoceanographical proxies based on deep-sea

760   benthic foraminiferal assemblage characteristics. Proxies in Late Cenozoic

761   Paleoceanography, Dev. Mar. Geol 1, 263–325.

762   Jouanneau, J.M., Garcia, C., Oliveira, A., Rodrigues, A., Dias, J.A., Weber, O., 1998. Dispersal

763   and deposition of suspended sediment on the shelf off the Tagus and Sado estuaries, SW

764   Portugal. Progress in Oceanography 42, 233–257.

765   Keigwin, L.D., Pickart, R.S., 1999. Slope water current over the Laurentian Fan on interannual

766   to millennial time scales. Science 286, 520–523.

767 Kitazato, H., Shirayama, Y., Nakatsuka, T., Fujiwara, S., Shimanaga, M., Kato, Y., Okada, Y.,

768   Kanda, J., Yamaoka, A., Masuzawa, T., Suzuki, K., 2000. Seasonal phytodetritus

769   deposition and responses of bathyal benthic foraminiferal populations in Sagami Bay,

770   Japan: preliminary results from "Project Sagami 1996–1999." Marine

771   Micropaleontology 40, 135–149.

772 Lamb, H.H., 1985. An approach to the study of the development of climate and its impact in

773   human affairs. Climate and History: Studies in Past Climates and Their Impact on Man

774   291–309.

775 Lebreiro, S.M., Francés, G., Abrantes, F.F.G., Diz, P., Bartels-Jónsdóttir, H.B., Stroynowski,

776   Z.N., Gil, I.M., Pena, L.D., Rodrigues, T., Jones, P.D., Nombela, M.A., Alejo, I., Briffa,

777   K.R., Harris, I., Grimalt, J.O., 2006. Climate change and coastal hydrographic response

778   along the Atlantic Iberian margin (Tagus Prodelta and Muros Ría) during the last two

779   millennia. The Holocene 16, 1003–1015.

780 Martins, M.V.A., Jouanneau, J.-M., Weber, O., Rocha, F., 2006. Tracing the late Holocene

781   evolution of the NW Iberian upwelling system. Marine Micropaleontology 59, 35–55.

782 Martins, M.V.A., Dubert, J., Jouanneau, J.-M., Weber, O., da Silva, E.F., Patinha, C., Dias,

783   J.M.A., Rocha, F., 2007. A multiproxy approach of the Holocene evolution of shelf–

784   slope circulation on the NW Iberian Continental Shelf. Marine Geology 239, 1–18.

785 Martins, M.V.A., Silva, F., Laut, L.M., Frontalini, F., Clemente, I., Miranda, P., Figueira, R.,

786   Sousa, S.H., Dias, J.M.A., 2015. Response of benthic foraminifera to organic matter

787   quantity and quality and bioavailable concentrations of metals in Aveiro Lagoon

788   (Portugal). Plos One. Doi: PONE-D-14-38075R1.

789 Mayewski, P.A., Rohling, E.E., Stager, J.C., Karlén, W., Maasch, K.A., Meeker, L.D.,

790   Meyerson, E.A., Gasse, F., van Kreveld, S., Holmgren, K., Lee-Thorp, J., Rosqvist, R.,

791   Rack, F., Staubwasser, M., Schneider, R.R., Steig, E.J., 2004. Holocene climate
792   variability. Quaternary Research 62, 243–255.

793   McCave, I.N., Hall, I.R., 2002. Turbidity of waters over the Northwest Iberian continental
794   margin. Progress in Oceanography 52, 299–313.

795   Mendes, I., Gonzalez, R., Dias, J.M.A., Lobo, F., Martins, V., 2004. Factors influencing recent
796   benthic foraminifera distribution on the Guadiana shelf (Southwestern Iberia). Marine
797   Micropaleontology 51, 171–192.

798   Mendes, I., Rosa, F., Dias, J.A., Schönfeld, J., Ferreira, Ó., Pinheiro, J., 2010. Inner shelf
799   paleoenvironmental evolution as a function of land–ocean interact ions in the vicinity
800   of the Guadiana River, SW Iberia. Quaternary International 221, 58–67.

801   Mendes, I., Dias, J.A., Schönfeld, J., Ferreira, Ó., 2012. Distribution of living benthic
802   foraminifera on the northern Gulf of Cadiz continental shelf. The Journal of
803   Foraminiferal Research 42, 18–38.

804   Mojtahid, M., Jorissen, F., Lansard, B., Fontanier, C., Bombled, B., Rabouille, C., 2009. Spatial
805   distribution of live benthic foraminifera in the Rhône prodelta: Faunal response to a
806   continental–marine organic matter gradient. Marine Micropaleontology 70, 177–200.

807   Mojtahid, M., Griveaud, C., Fontanier, C., Anschutz, P., Jorissen, F.J., 2010a. Live benthic
808   foraminiferal faunas along a bathymetrical transect (140–4800m) in the Bay of Biscay
809   (NE Atlantic). Revue de micropaléontologie 53, 139–162.

810   Mojtahid, M., Jorissen, F., Lansard, B., Fontanier, C., 2010b. Microhabitat selection of benthic
811   foraminifera in sediments off the Rhône River mouth (NW Mediterranean). The Journal
812   of Foraminiferal Research 40, 231–246.

813   Murray, J.W., 2006. Ecology and applications of benthic foraminifera. Cambridge University
814   Press.

815   Oliveira, A., Santos, A.I., Rodrigues, A., Vitorino, J., 2007. Sedimentary particle distribution

816   and dynamics on the Nazaré canyon system and adjacent shelf (Portugal). Marine

817   Geology 246, 105–122.

818   Ortega, P., Lehner, F., Swingedouw, D., Masson-Delmotte, V., Raible, C.C., Casado, M., Yiou,

819   P., 2015. A model-tested North Atlantic Oscillation reconstruction for the past

820   millennium. Nature 523, 71–74.

821   Owens, N.J.P., 1985. Variations in the natural abundance of 15 N in estuarine suspended

822   particulate matter: a specific indicator of biological processing. Estuarine, Coastal and

823   Shelf Science 20, 505–510.

824   Peliz, Á., Rosa, T.L., Santos, A.M.P., Pissarra, J.L., 2002. Fronts, jets, and counter-flows in the

825   Western Iberian upwelling system. Journal of Marine Systems 35, 61–77.

826   Peters, K.E., Sweeney, R.E., Kaplan, I.R., 1978. Correlation of carbon and nitrogen stable

827   isotope ratios in sedimentary organic matter 1. Limnology and Oceanography 23, 598–

828   604.

829   Prieto, L., Navarro, G., Rodríguez-Gálvez, S., Huertas, I.E., Naranjo, J.M., Ruiz, J., 2009.

830   Oceanographic and meteorological forcing of the pelagic ecosystem on the Gulf of

831   Cadiz shelf (SW Iberian Peninsula). Continental Shelf Research 29, 2122–2137.

832   Relvas, P., Barton, E.D., Dubert, J., Oliveira, P.B., Peliz, A., Da Silva, J.C.B., Santos, A.M.P.,

833   2007. Physical oceanography of the western Iberia ecosystem: latest views and

834   challenges. Progress in Oceanography 74, 149–173.

835   Rodrigues, T., Grimalt, J.O., Abrantes, F.G., Flores, J.A., Lebreiro, S.M., 2009. Holocene

836   interdependences of changes in sea surface temperature, productivity, and fluvial inputs

837   in the Iberian continental shelf (Tagus mud patch). Geochemistry, Geophysics,

838   Geosystems 10.

839   Rosa, F., Fatela, F., Drago, T., 2007. Late Holocene benthic foraminiferal records in the
840   continental shelf off Douro River (NW Portugal): evidences for productivity and
841   sedimentary relationships. Thalassas 23, 19–31.

842   Schmidt, F., Hinrichs, K.-U., Elvert, M., 2010. Sources, transport, and partitioning of organic
843   matter at a highly dynamic continental margin. Marine Chemistry 118, 37–55.

844   Schönfeld, J., 2002. A new benthic foraminiferal proxy for near-bottom current velocities in
845   the Gulf of Cadiz, northeastern Atlantic Ocean. Deep Sea Research Part I:
846   Oceanographic Research Papers 49, 1853–1875.

847   Schubert, C.J., Calvert, S.E., 2001. Nitrogen and carbon isotopic composition of marine and
848   terrestrial organic matter in Arctic Ocean sediments:: implications for nutrient
849   utilization and organic matter composition. Deep Sea Research Part I: Oceanographic
850   Research Papers 48, 789–810.

851   Stuiver, M., Reimer, J., 1993. Extended 14C data base and revised CALIB 3.014 C age
852   calibration program. EDITORIAL COMMENT 35, 215–230.

853   Stuut, J.-B.W., Temmesfeld, F., De Deckker, P., 2014. A 550 ka record of aeolian activity near
854   North West Cape, Australia: inferences from grain-size distributions and bulk chemistry
855   of SE Indian Ocean deep-sea sediments. Quaternary Science Reviews 83, 83–94.

856   Suhr, S.B., Pond, D.W., Gooday, A.J., Smith, C.R., 2003. Selective feeding by benthic
857   foraminifera on phytodetritus on the western Antarctic Peninsula shelf: evidence from
858   fatty acid biomarker analysis. Marine Ecology Progress Series 262, 153–162.

859   Swingedouw, D., Ortega, P., Mignot, J., Guilyardi, E., Masson-Delmotte, V., Butler, P.G.,
860   Khodri, M., Séférian, R., 2015. Bidecadal North Atlantic ocean circulation variability
861   controlled by timing of volcanic eruptions. Nature communications 6.

862   Taylor, S.R., 1965. The application of trace element data to problems in petrology. Phys. Chem.
863   Earth 6, 133–213.

864 Tilstone, G.H., Figueiras, F.G., Lorenzo, L.M., Arbones, B., 2003. Phytoplankton composition,

865 photosynthesis and primary production during different hydrographic conditions at the

866 Northwest Iberian upwelling system. Marine Ecology Progress Series 252, 89–104.

867 Tjallingii, R., Röhl, U., Kölling, M., Bickert, T., 2007. Influence of the water content on X-ray

868 fluorescence core-scanning measurements in soft marine sediments. Geochemistry,

869 Geophysics, Geosystems 8.

870 Trigo, R.M., Pozo-Vàzquez, D., Osborn T.J., Castro-Díez, Y., Gámiz-Fortis, S., Esteban-Parra,

871 M.J., 2004. North Atlantic Oscillation influence on precipitation, river flow and water

872 resources in the Iberian Peninsula. International Journal Of Climatology 24, 925–944.

873 Trouet, V., Esper, J., Graham, N.E., Baker, A., Scourse, J.D., Frank, D.C., 2009. Persistent

874 positive North Atlantic Oscillation mode dominated the medieval climate anomaly.

875 Science 324, 78–80.

876 Vale, C., Sundby, B., 1987. Suspended sediment fluctuations in the Tagus estuary on semi-

877 diurnal and fortnightly time scales. Estuarine, Coastal and Shelf Science 25, 495–508.

878 van Aken, H.M., 2000a. The hydrography of the mid-latitude northeast Atlantic Ocean: I: The

879 deep water masses. Deep Sea Research Part I: Oceanographic Research Papers 47, 757–

880 788.

881 van Aken, H.M., 2000b. The hydrography of the mid-latitude Northeast Atlantic Ocean: II: The

882 intermediate water masses. Deep Sea Research Part I: Oceanographic Research Papers

883 47, 789–824.

884 Vitorino, J., Oliveira, A., Jouanneau, J.M., Drago, T., 2002a. Winter dynamics on the northern

885 Portuguese shelf. Part 2: bottom boundary layers and sediment dispersal. Progress in

886 Oceanography 52, 155–170.

887 Vitorino, J., Oliveira, A., Jouanneau, J.M., Drago, T., 2002b. Winter dynamics on the northern

888 Portuguese shelf. Part 1: physical processes. Progress in Oceanography 52, 129–153.

889   Wanner, H., Brönniman, S., Casty, C., Gyalistras, D., Luterbacher, J., Schmutz, C., Stephenson,

890   D.B., Xoplaki, E., 2001. North Atlantic Oscillation – concept and studies. Surveys in

891   Geophysics 22, 321–381.

892   Warden, L., Kim, J.-H., Zell, C., Vis, G.-J., de Stigter, H., Bonnin, J., Damsté, J.S.S., 2016.

893   Examining the provenance of branched GDGTs in the Tagus River drainage basin and

894   its outflow into the Atlantic Ocean over the Holocene to determine their usefulness for

895   paleoclimate applications. Biogeosciences 13, 5719-5738.

896   Weltje, G.J., Tjallingii., R, 2008. Calibration of XRF core scanners for quantitative geochemical

897   logginig of sediment cores: Theory and application. Earth and Planetary Science

898   Letters274, 423-438.

899   Ziegler, M., Jilbert, T., de Lange, G.J., Lourens, L.J., Reichart, G.-J., 2008. Bromine counts

900   from XRF scanning as an estimate of the marine organic carbon content of sediment

901   cores. Geochemistry. Geophysics. Geosystems 9.

902

903   **Figures**
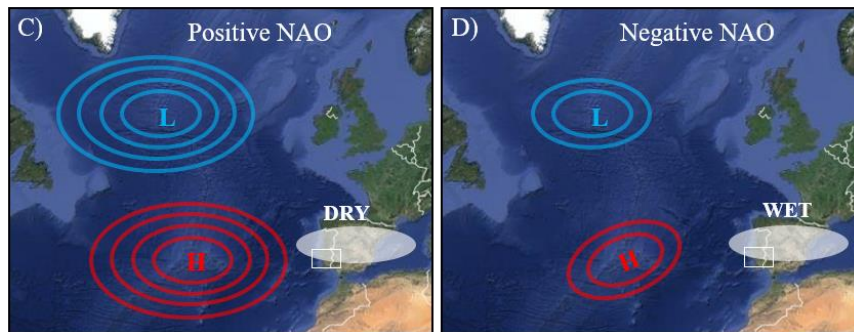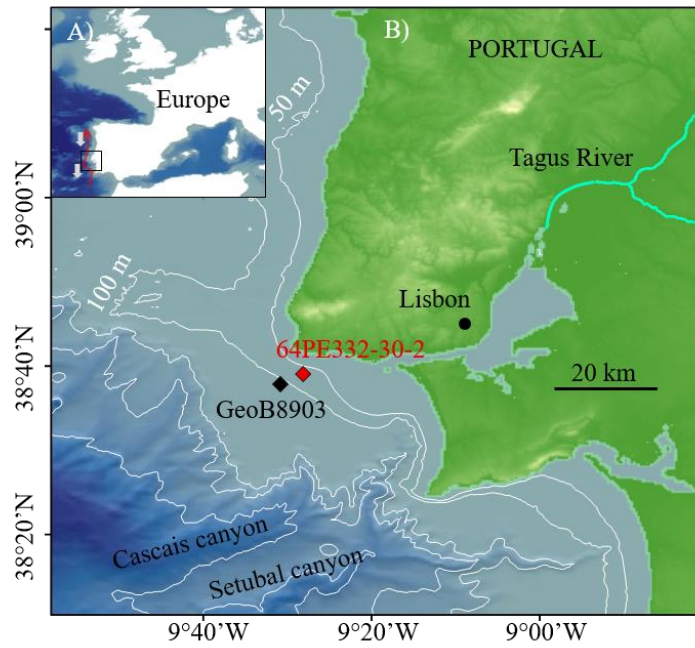
Fig. 1. A) General location map of the study area, with a schematic representation of the Portugal Coastal Counter Current (red arrow) and the ENACW (grey arrows). B) Detailed map of the core locations considered in this study. Red diamond: piston cores 64PE332-30-2, this study; black diamond: GeoB8903 (Abrantes et al., 2008). C) Positive and D) Negative phase of NAO with L = Iceland low-pressure system and H = Azores high-pressure system.
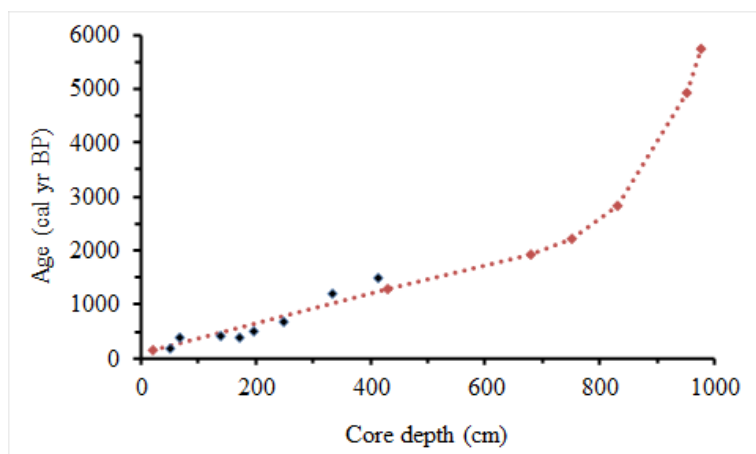
911

912
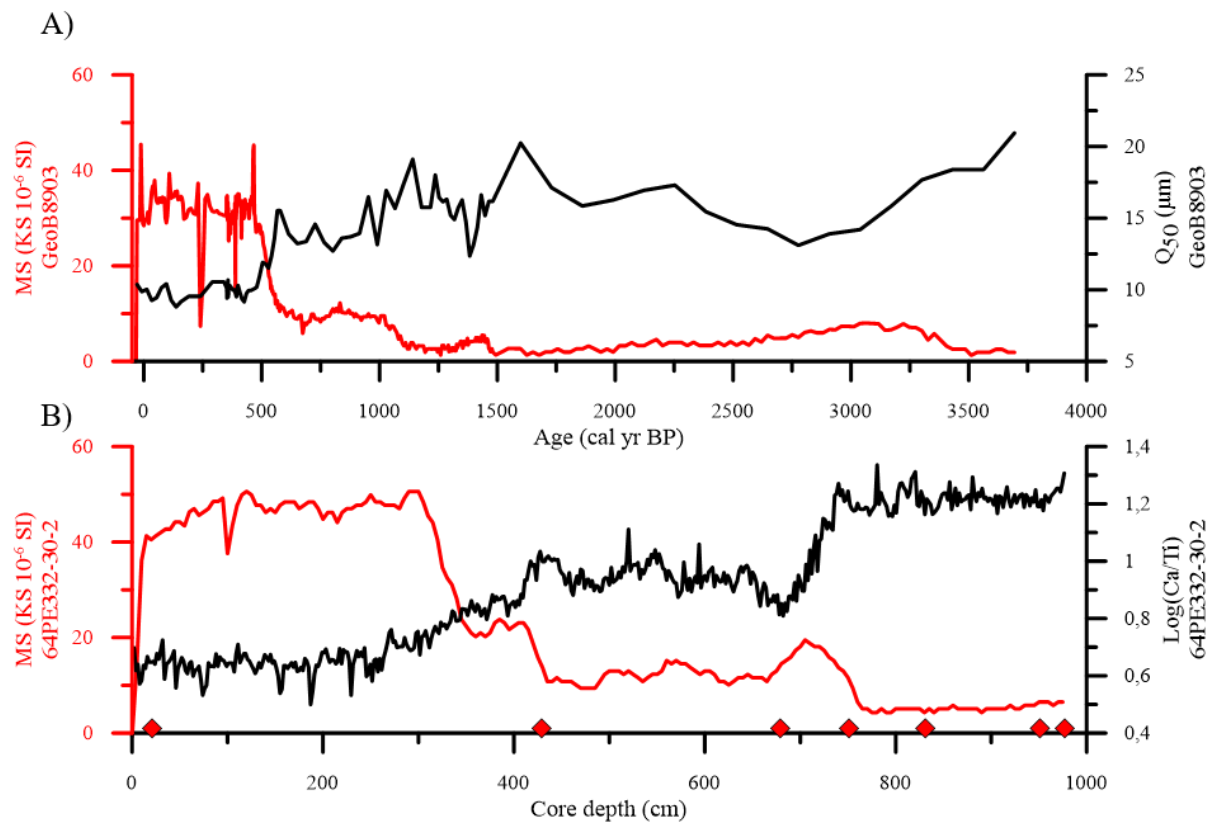
Fig. 2. Comparison of Ca/Ti and magnetic susceptibility (MS) of Core 64PE332-30-2 with grain size (Q_{50}) and MS from Core GeoB 8903 (Abrantes et al., 2008; Alt-Epping et al., 2009). Red diamonds represent ^{14}C data points.

916

917

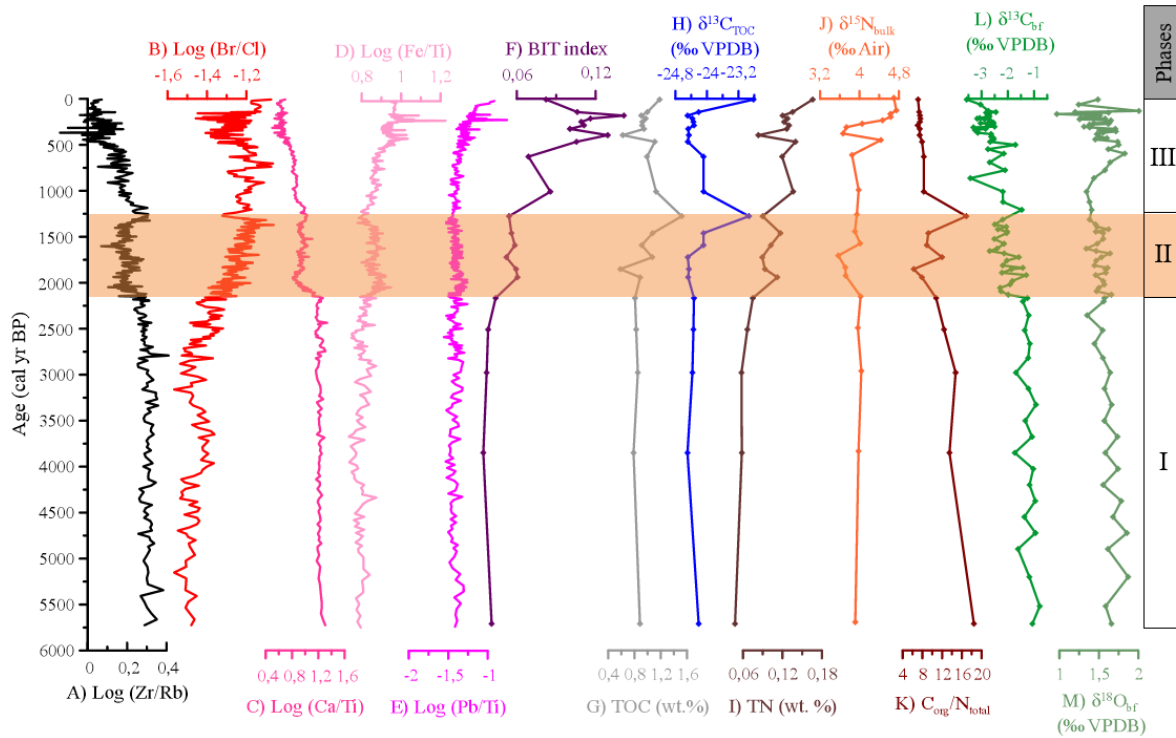Fig. 3. Age model of Core 64PE332-30-2 based on AMS ^{14}C data (Table 1). Blue diamonds represent the ^{14}C data points of GeoB 8903.
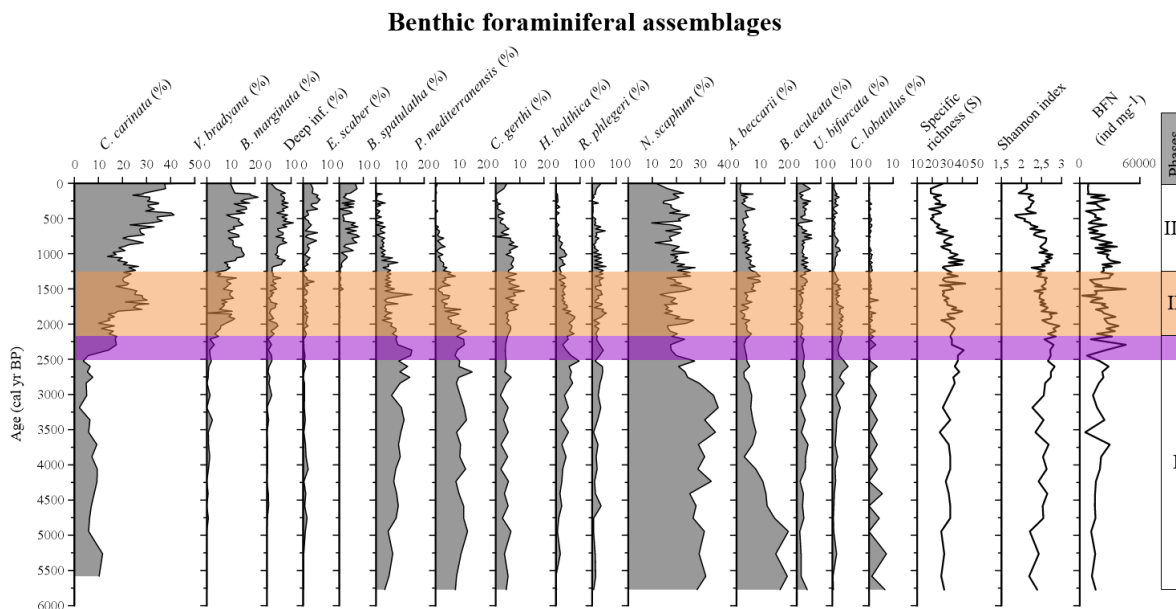
920

Fig. 4. Distribution of environmental parameters for the last 5750 years. XRF data: A) Zr/Rb, B) Br/Cl, C) Ca/Ti, D) Fe/Ti and E) Pb/Ti. Organic measures: F) TN, G) TOC, H) C/N ratio, I) $\delta^{15}N_{bulk}$, J) $\delta^{13}C_{TOC}$, and K) BIT index. Carbonate isotopes L) $\delta^{13}C_{bf}$ and M) $\delta^{18}O_{bf}$ analyzed for the species *N. scaphum*. The orange square indicates the limits of the three phases.

Fig. 5. Distribution of major species of benthic foraminifera (>5%) and specific richness from the 101 samples of Core 64PE332-30-2 for the last 5750 years. Deep inf. = *G. affinis* + *C. oolina*. The orange square indicates the limits of the three phases, and the purple square follows the main change of the faunal distribution.

41

933
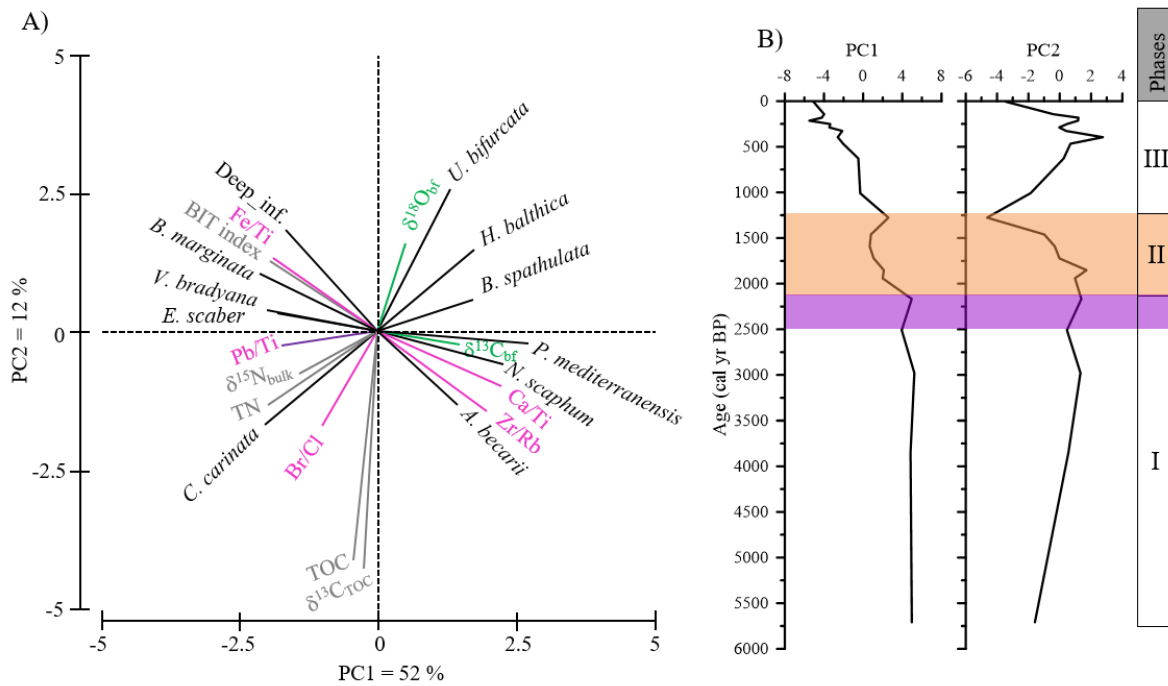
Fig. 6.A) PCA based on the major species percentages (in black), XRF data (in pink), organic compounds (in grey), and benthic foraminiferal isotopes (in green). B) Score profiles of PC1 and PC2 as a function of time. The orange square indicates the limits of the three phases, and the purple square follows the main change of the faunal distribution.

938
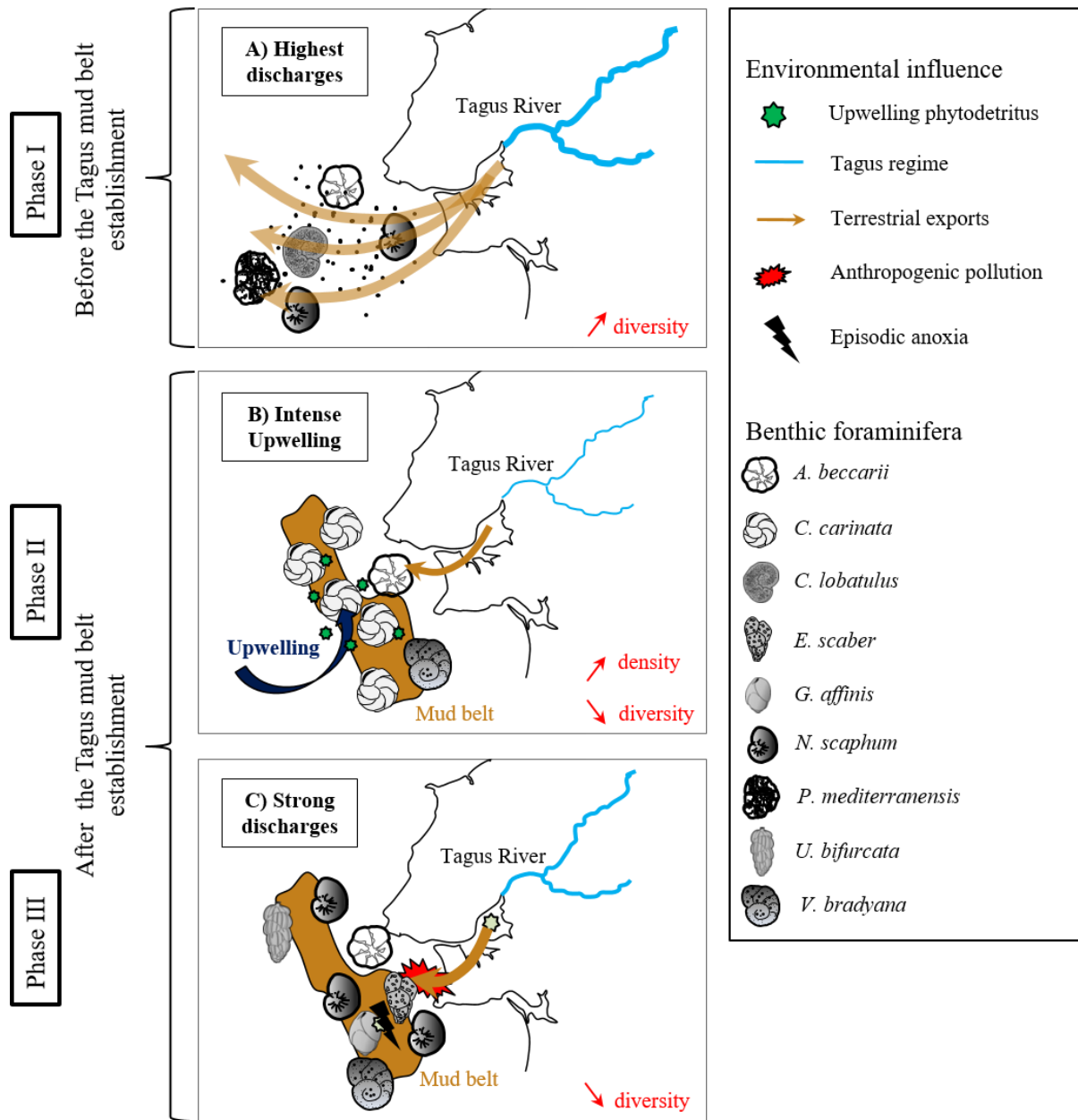
Fig. 7. Schematic representation of the three modes associated with the Tagus mud belt establishment, Tagus River regime, and upwelling intensity. A) First phase, characterized by very high Tagus River discharge. B) Second phase: mud belt establishment and very intense upwelling activity. C) Alternating periods of strong upwelling activity and high Tagus River discharge.

944

Key taxa	Faunal diversity	Benthic Productivity (– → +)	Tagus vs. Upwelling	Climatic Period	Phase
C. carinata, E. scabra, S. karreriana	Contaminant-tolerant species		High upwelling influence	PWP	III
V. bradyana, A. beccarii, G. affinis, C. oolina	Contaminant-tolerant species		↗ Tagus Discharges	LIA	III
C. carinata, B. marginata	↘↘ diversity		Upwelling and Tagus alternances	MWP	III
A. beccarii, N. scaphum, C. carinata	↗ diversity ↘ diversity		High upwelling influence	DA	II
N. scaphum, V. bradyana	↘↘ diversity		Mud Tagus exports	RP	II
C. carinata	Stable diversity		↘ Tagus dynamic	SA	I
A. beccarii, P. mediterranensis, N. scaphum	↗↗ diversity		High Tagus regime	SB	I

Tagus discharges (– → +)

Fig. 8. Summary of the paleoenvironmental evolution of the Tagus River during the last 5750 years. RP = Roman Period, DA = Dark Ages, MWP = Medieval Warm Period, LIA = Little Ice Age, PWP = Present Warm Period, SA = Sub-Atlantic Period, SB = Subboreal Period. The orange square indicates the limits of the three phases, and the purple square follows the main change of the faunal distribution.
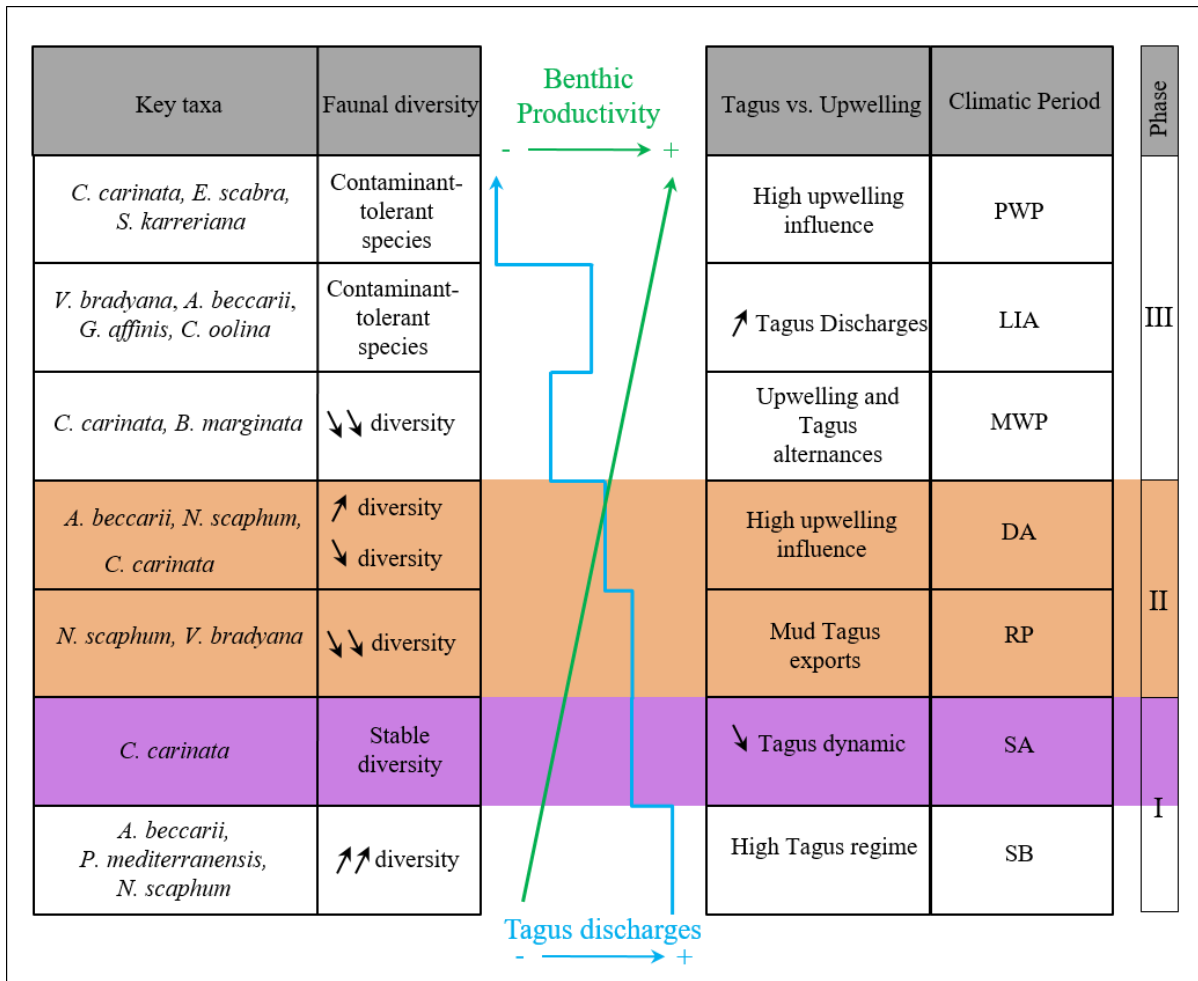
953   Table 1. ^{14}C AMS dates of cores GeoB 8903 and 64PE332-30-2.

Sediment core	Lab no.	Core depth interval [cm]	Mean depth in core [cm]	Uncorrected AMS ^{14}C ages [cal yr BP]	Analytical error (±1σ) [yrs]	Ages (ΔR = 0 yr)(±2σ) [cal yr BP]	Ages [cal yr BP]	Analyzed material	Reference
GeoB 8903	KIA30888	52-53	51	210	35	138-223	182	Foraminifera	Alt-Epping et al. (2009)
GeoB 8903	KIA30890	65-70	69	335	55	300-501	394	Foraminifera	Alt-Epping et al. (2009)
GeoB 8903	-	139-141	140	360	25	349-456	425	Foraminifera	Alt-Epping et al. (2009)
GeoB 8903	-	171-173	172	285	30	314-408	381	Foraminifera	Alt-Epping et al. (2009)
GeoB 8903	-	198-199	198	360	45	423-498	487	Foraminifera	Alt-Epping et al. (2009)
GeoB 8903	-	248-249	248	735	30	657-726	679	Foraminifera	Alt-Epping et al. (2009)
GeoB 8903	-	333-334	333	1260	35	1121-1282	1210	Foraminifera	Alt-Epping et al. (2009)
GeoB 8903	-	413-414	413	1600	40	1390-1567	1478	Foraminifera	Alt-Epping et al. (2009)
64PE332-30-2	BETA 348791	20-22	21	500	30	41 - 235	138	Gastropod	Warden et al. (2016)
64PE332-30-2	BETA 348792	428-430	429	1730	30	1219 - 1350	1284.5	Foraminifera	Warden et al. (2016)
64PE332-30-2	BETA 348793	678-680	679	2320	30	1848 - 2033	1940.5	Gastropod	Warden et al. (2016)
64PE332-30-2	VERA-51394	750-752	751	2530	70	2122-2293	2207.5	Gastropod	This study
64PE332-30-2	VERA-51395	830-832	831	3060	70	2749-2902	2825.5	Gastropod	This study
64PE332-30-2	VERA-51396	950-952	951	4690	70	4831-5007	4919	Gastropod	This study
64PE332-30-2	BETA 317911	976-978	977	5370	30	5644 - 5850	5747	Shell fragments	Warden et al. (2016)

954   Note that ^{14}C data from GeoB 8903 were from Alt-Epping et al. (2009) and reconverted using the CALIB V0.6 with the Marine13 calibration
955   curve (Stuiver and Reimer, 1993).